PERFORMANCE OF A TRANSMIT DELAY SCHEME IN DIGITAL
SIMULCAST ENVIRONMENT

A THESIS SUBMITTED TO
THE GRADUATE SCHOOL OF NATURAL AND APPLIED SCIENCES
OF
MIDDLE EAST TECHNICAL UNIVERSITY

BY

AYFER ÖZGÜR

IN PARTIAL FULFILLMENT OF THE REQUIREMENTS
FOR
THE DEGREE OF MASTER OF SCIENCE
IN
ELECTRICAL AND ELECTRONICS ENGINEERING

JULY 2004

Approval of the Graduate School of Natural and Applied Sciences

_____

Prof. Dr. Canan Özgen

Director

I certify that this thesis satisfies all the requirements as a thesis for the degree of Master of Science

_____

Prof. Dr. Mübeccel Demirekler

Head of Department

This is to certify that we have read this thesis and that in our opinion it is fully adequate, in scope and quality, as a thesis for the degree of Master of Science.

_____

Prof. Dr. Yalçın Tanık

Supervisor

Examining Committee Members

Prof. Dr. Rüyal Ergül	(METU, EE)	_____
Prof. Dr. Yalçın Tanık	(METU, EE)	_____
Assoc. Prof. Dr. Melek Yücel	(METU, EE)	_____
Prof. Dr. Mete Severcan	(METU,EE)	_____
Prof. Dr. Mehmet Şafak	(Hacettepe University,EE)	_____

I hereby declare that all information in this document has been obtained and presented in accordance with academic rules and ethical conduct. I also declare that, as required by these rules and conduct, I have fully cited and referenced all material and results that are not original to this work.

Name, Last name : Ayfer ÖZGÜR

Signature :

ABSTRACT

PERFORMANCE OF A TRANSMIT DELAY SCHEME IN DIGITAL SIMULCAST ENVIRONMENT

ÖZGÜR, Ayfer

M.Sc., Department of Electrical and Electronics Engineering

Supervisor: Prof. Dr. Yalçın TANIK

July 2004, 88 pages

Simulcasting is a spectrally efficient wide area coverage technique that can be advantageous in private mobile radio applications such as emergency services. In a simulcast network, multiple base stations broadcast the same information on a single nominal carrier frequency, causing severe multipath interference at a receiver in the overlap region of several neighboring base stations. In this thesis, we introduce a transmit delay scheme for simulcast networks and investigate the performance of the scheme in LOS and Rayleigh fading environments. In this scheme a relative transmit delay is introduced between neighboring base stations to extend the differential delay between different paths in the overlap regions, from the order of the carrier period to the order of the symbol period, thus transform RF carrier interference into ISI. The receiver employs MLSE to obtain diversity gain from ISI. The performance of the system is evaluated using analytical bounds and simulations carried out for an MLSE

based $\pi/4$ DQPSK receiver and the results show that the proposed scheme operates succesfully, turning destructive interference disadvantage into a multipath diversity advantage, provided that a sufficient delay is used between the base stations. The "sufficient" delay value is determined by considering the coverage properties of the scheme and is in fact "optimum", since more than sufficient transmit delays result in useless increased receiver complexity. We provide our results using parameters for the TETRA system, however, the results of the work can readily be used for other systems.

Keywords: Simulcasting, transmit delay scheme, MLSE, $\pi/4$ DQPSK, TETRA

ÖZ

GÖNDERMEDE GECİKMELERE DAYALI BİR DÜZENİN AYNI FREKANS ÜZERİNDEN YAYIN YAPAN AĞLAR İÇİN BAŞARIMI

ÖZGÜR, Ayfer

Yüksek Lisans, Elektrik ve Elektronik Mühendisliği Bölümü

Tez Yöneticisi: Prof. Dr. Yalçın TANIK

Temmuz 2004, 88 sayfa

Aynı frekans üzerinden yayın yapmak geniş alanları kapsamak için kullanılan, tayf kullanımı açısından verimli bir yöntemdir ve acil durum servisleri gibi özel gezgin radyo uygulamalarında kullanışlı olabilmektedir. Aynı frekans üzerinden yayın yapan bir ağda birden fazla baz istasyonu aynı bilgiyi tek bir nominal frekans üzerinden yayınlamakta ve bu da birkaç baz istasyonunun kapsama alanlarının örtüştüğü bölgelerdeki alıcılarda ciddi bir girişim problemine yol açmaktadır. Bu tezde, aynı frekans üzerinden yayın yapan ağlar için göndermede gecikmelere dayalı bir düzen sunulmakta ve bu düzenin vericiye açık görüş olan ve Rayleigh dalgalanan ortamlarda başarımı araştırılmaktadır. Bu düzende, farklı baz istasyonlarından gelen sinyaller arasında örtüşme bölgelerindeki gecikmeyi, RF taşıyıcısının periyodu mertebesinden sembol periyodu mertebesine çıkartmak, yani taşıyıcılar arasındaki

girişimi sembol girişimine çevirmek için, komşu baz istasyonlarının birbirlerine göre gecikmeli yayın yapmaları sağlanmaktadır. Sembol girişiminden çeşitlilik kazancı sağlamak için alıcılarda en büyük olabilirlikli diziyi kestiren bir yapı kullanılmaktadır. Sistemin başarımı teorik sınırlar ve en olası diziyi kestiren $\pi/4$ DQPSK alıcı için benzetimler yapılarak çalışılmakta ve sonuçlar, önerilen düzenin, baz istasyonları arasında yeterli gecikmenin kullanılması durumunda yıkıcı girişim dezavantajını çeşitlilik kazancına dönüştürerek başarılı bir şekilde çalıştığını göstermektedir. "Yeterli" olan gecikme değeri, düzenin kapsama özellikleri göz önünde bulundurularak belirlenmektedir ve göndermedeki gereğinden fazla gecikmeler alıcı karmaşıklığını fayda sağlamaksızın arttıracağından aslında "en uygun"dur. Sonuçlar TETRA parametreleri kullanılarak elde edilmiş olmasına karşın rahatlıkla başka sistemler için genişletilebilir.

Anahtar Sözcükler: Aynı frekans üzerinden yayın yapan ağlar, göndermede gecikmelere dayalı düzen, en büyük olabirlikli dizinin kestirimi, $\pi/4$ DQPSK, TETRA

To My Parents,

for their love and support

ACKNOWLEDGMENT

TABLE OF CONTENTS

LIST OF TABLES

LIST OF FIGURES

CHAPTER 1

INTRODUCTION

Mobile radio networks for wide area coverage usually include more than one base station. The reason is quite obvious: A single base station in such network can only serve a limited area. Enlarging the coverage area of a single base station will require extra transmit power in both the base station and the mobiles. Likewise covering rugged terrains where it is likely that the transmitter is shadowed in certain regions will also require the installation of additional base stations. Thus, to support large areas, the infrastructure needs to consist of many base station sites regularly spread over the intended service area, forming the so-called cellular planned networks.

Conventional cellular network planning strategies assign different frequencies to neighboring base stations to avoid interference at the mobile from surrounding base stations. Limitations of available frequency allocations for mobile radio communications dictate efficient use of available frequency spectrum. A fundamental approach to achieve high spectrum utilization is to reuse the allocated frequencies in geographically separated areas. When reusing the spectrum, the base stations using the same channel should be separated by a minimum distance determined by propagation variables such that there is no risk of interference. This minimum distance is called the reuse distance. An illustration of a cellular network with frequency reuse strategy is shown in Figure-1 A [1]. This type of frequency planning is very important in almost all radio systems.

For service areas with heavy traffic load, cellular network planning with frequency reuse strategy is often necessary although the required service area may not be so large. However some private/professional mobile radio applications (PMR) such as
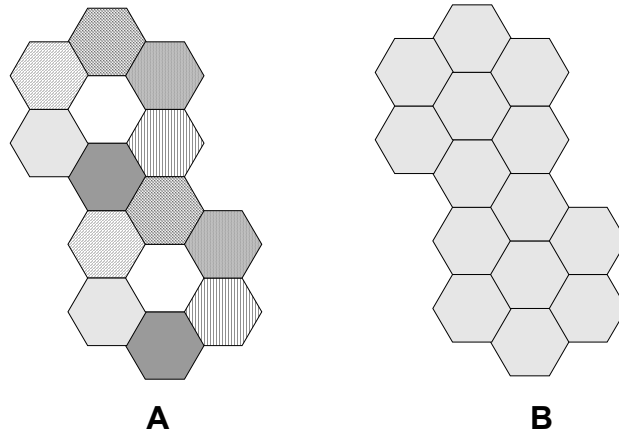
Figure-1 A) A conventional network B) A simulcast network.
Different patterns represent different frequencies.

emergency services including police, ambulance and fire services may have low
traffic load but require large service areas. Simulcasting is widely used in these
applications to achieve total area coverage. In simulcasting the same information is
simultaneously broadcasted over a multi station system operating on a single nominal
carrier frequency. The frequency assignment in a simulcast network is also shown in
Figure-1B. Since all sites on the network use the same carrier frequency, spectrum
utilization is enhanced. Besides spectral efficiency, implementing PMR systems with
simulcast transmission has other advantages [1, 2]. The operation of all base station
sites on a single carrier frequency eliminates the need for handoff or switching from
one channel to another while the mobile is roaming through the service area.
Additionally, mobile-to-mobile communication is easily achieved by feeding the
signal to all base station sites, eliminating the need for mobile tracking management.
These two advantages result in operating efficiency.

Simulcasting also suggests improved coverage properties. The service area can be of
irregular shape and extra transmitters (gap fillers) operating in simulcast mode may
be placed to improve coverage in areas that are not properly served by the main base
station. The gap-fillers do not require any additional frequency bands. The spatial
diversity inherent in simulcasting is another advantage that reduces the effects of

fading in mobile environment. Moreover, the simulcast network can be designed to include regularly spread low power transmitter sites. Thus the total radiated power in a simulcast network might be much less than the case when high power transmitters are used to cover the same area. This point is illustrated in Figure-2 [1]. Failure of a base station is less serious in this case since, a failure of a low power base station will affect only a small area and the simulcast from neighboring base stations will provide a degree of fill-in coverage in the service area of the failing transmitter site. Simulcasting also allows lower elevation sites. Low power transmitters and low elevation sites could give dramatic reductions in frequency reuse distance. Note that now the frequency reuse distance refers to the minimum separation required between two networks operating on the same nominal carrier frequency.

Another application of simulcast may be to establish a number of common channels that should broadcast the same information to an area larger than the cell associated with a single base station. Dispatching systems and radio paging systems are examples where the broadcast feature is employed. A typical scenario [3], where this is useful, is a countywide police operation, which involves large number of mobiles. All mobiles must be able to listen to the communication with the control office in order to be aware of the current state of the operation.   In these applications, simulcasting may be used to provide a common channel over the whole network while maintaining spectral efficiency.

[†] Since we will be interested only in the downlink transmission in this thesis, the words 'transmitter' and 'base station' will be used interchangeably throughout the text. The same is valid for words 'receiver' and 'mobile station' or 'mobile terminal'. When the transmission from a mobile station or reception of the base station is referred, it will be explicitly indicated.
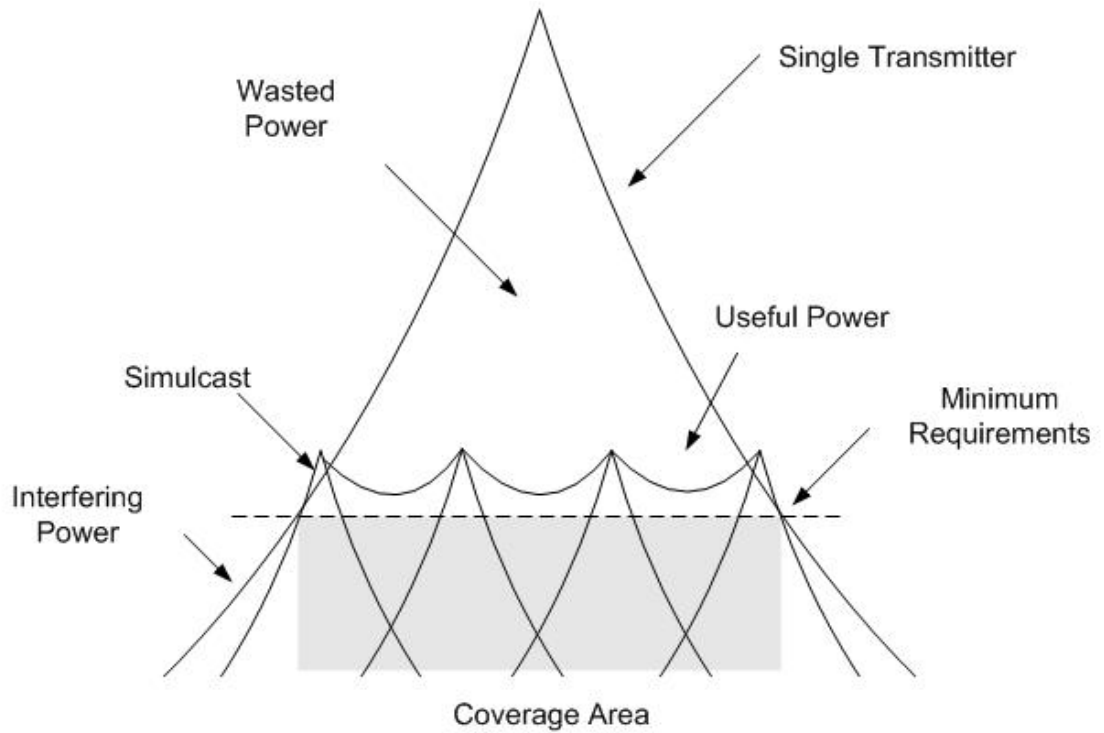
Figure-2 Received power for a single transmitter system and simulcast network

1.1   Background

In this part, we will briefly overview work done in the literature related to the aim of this thesis. In the following section, we will overview different simulcasting techniques. Since the simulcasting technique is, in effect, a transmitter space diversity scheme we will overview spatial transmit diversity techniques in Section 1.2. In the last section of this chapter we will give the scope of this thesis and discuss the relation of various work introduced in the previous sections with the aim of this thesis.

1.1.1 Simulcasting Techniques

The main problem with simulcasting is the artificial multi-path that occurs in overlap regions. A mobile station in the overlap region receives two or more signals from different base stations, which arrive with relative delays. When the arrival times of the different rays are of the same order of magnitude as the duration of the transmitted symbols, successive symbols are smeared together. This effect is often referred to as intersymbol interference (ISI). For paths, where the time difference is comparable to the period of the radio frequency (RF) carrier another effect results. Superposition of many waves with different phases here gives a spatial interference pattern, with narrow gaps of extremely low signal power, so called deep fades. The spatial interference pattern is illustrated in Figure-3. Those deep fades are located at distances comparable to the wavelength of the RF carrier and the signal power in a fade can be so low that communication becomes impossible [4]. These deep fades are inherent to the structure of simulcasting and cannot be overcome by increasing transmitter power. Techniques to counter these problems are essential for the simulcast system to operate.
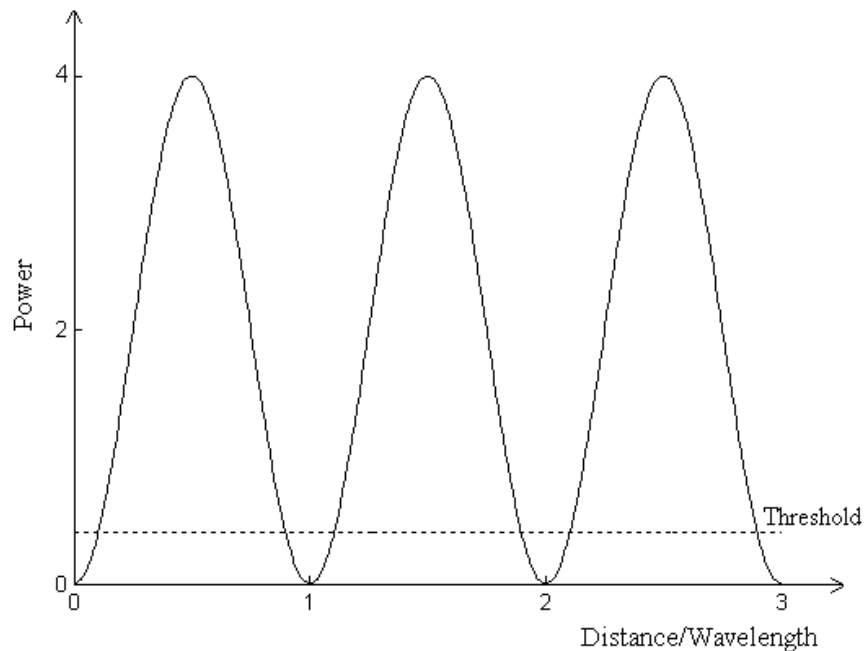
Figure-3 Interference due to artificial multi path effect in simulcasting

5

From another point of view, the artificial multi-path in simulcasting is, in effect, a transmitter space-diversity scheme. If the individual paths can be distinguished at the receiver, the above problems may be solved to provide diversity gain to the receiver. Diversity gain will reduce the effects of fading in mobile environment.

Simulcasting is quite often referred as quasi-synchronous transmission since this is one of the most commonly employed implementations of simulcasting. In quasi-synchronous transmission small frequency offsets (a few hertz to a few hundred hertz) are allowed between RF carriers of different base stations. The interference pattern illustrated in Figure-3 is still present in the overlap areas, but due to the slight frequency offset allowed between the RF carriers, the deep fades change position with time. A static terminal will observe a slowly fading signal.

The quasi-synchronous transmission is designed more to circumvent the problems imposed by simulcasting than to actually solve them. The main purpose is to design a simulcast network where simple receivers can work. The technique has been employed in analogue systems in the last years and simulations have been performed to investigate the performance of the technique with digital systems, such as the new Pan European PMR system, TETRA. TETRA simulation results for quasi-synchronous transmission show that the differential delays between different rays in the overlap area severely degrade the performance due to ISI and should be kept less than 0.25 of the symbol period [5, 6, 7]. This restriction limits the data transmission rate, base station separation and size of the coverage area with quasi-synchronous transmission since the overlap area should be designed so narrow that the differential delay does not exceed a quarter of the symbol period. Hence, often equalization is required to achieve acceptable error ratios with relatively high data rates such as 36 kbps in TETRA. However, employing an equalizer at the receiver is contradiction to the basic motivation for implementing quasi-synchronous transmission since the basic motivation was to employ simple receivers at the mobiles.

Another simulcasting technique suggested in 1991 by Wittneben [3] is closely related to the aim of this thesis. In [3], a scheme that uses different FIR filters at the base stations is suggested. The coefficients of the FIR filters are chosen such that a

necessary condition to obtain diversity gain at the receiver is satisfied. For example, a two-base station scheme where the two base stations transmit the same information-bearing signal but one of the base stations is delayed by one symbol period relative to the other, corresponds to a special choice of the FIR filter coefficients. The scheme introduces intended ISI in the received signal and equalization is employed at the mobiles to obtain diversity gain against ISI. The scheme is attractive because, at the expense of increased receiver complexity, it does strictly preserve the bandwidth requirement. Increased complexity arises from the need for an equalizer in the receiver. However, performance evaluations of TETRA for example, have shown that equalization is already essential in order to cope with the extreme propagation conditions of hilly terrains or quasi-synchronous environments [8]. This technique utilizes an equalizer, which is anyway present in the mobile receiver to provide diversity benefit in fading environment.

In [9], the use of an equalizer at the receiver is suggested to handle the problem of ISI in simulcasting. The author investigates the performance of receivers with a minimum mean squared error (MMSE) linear equalizer and a decision feedback equalizer in simulcast environment and independently from [3] finds out that introducing a couple of symbol delays between the two base stations improves the performance. This result is the special case of the scheme suggested by Wittneben [3].

Some other simulcasting techniques implicitly or explicitly utilize orthogonalization so that the individual paths are distinguished at the receiver and diversity gain is obtained. Orthogonalization is achieved by using either different modulation indexes or different frequency slots at different base stations. All these methods increase the bandwidth requirement contradicting with the basic motivation of spectral efficiency in implementing simulcast networks.

1.1.2   Spatial Transmit Diversity Techniques

In spatial transmit diversity, or transmit diversity in short as referred in the rest of this work, multiple transmit antennas at the base station transmit the same information to the mobile providing several independent paths from the base station to the mobile. The objective is to combine multiple signals by appropriate signal processing at the receiver and reduce the effects of excessively deep fades. Diversity schemes can minimize the effects of fading since deep fades seldom occur simultaneously during the same time intervals on two or more paths.

At this point, one thing is worth mentioning. In general, transmit diversity techniques aim to supply different replicas of the transmitted signal to the receiver. That is, the receiver should be able to distinguish different signals coming from different transmit antennas. In order to achieve this aim, these techniques basically employ different parameters at different transmit antennas. However it should be noted that even if all transmit antennas were to transmit identical signals with completely identical parameters, the combination of fading signals at the receiver would already be, most of the time, constructive [10]. That is, without employing any transmit diversity technique at the antennas, thus simply transmitting the signal form more than one transmit antenna, the simple addition of two or more fading signals at the receiver is constructive with high probability and will increase the mean power experienced at the mobile. When saying that a transmit diversity technique is able to provide diversity gain to the receiver, we mean that it enables the receiver to distinguish individual signals coming from different paths and by means of appropriate combining schemes provides a further gain to the receiver over the gain obtained by simple addition of several paths.

Notice that transmit diversity techniques and base station simulcasting are similar in the sense that both systems involve multiple paths from transmit antennas to the mobile. In transmit diversity, multiple transmit antennas are located on a single base station and are only several wavelength apart. Propagation delay differences between different paths are negligible in this case. In simulcasting, the transmit antennas are located on different base stations and propagation delay differences between

8

different paths are inevitable throughout the network, coming out as an important parameter that determines the coverage properties of a simulcast network.

The scheme suggested by Wittneben [3] for simulcasting has also been suggested for transmit antenna diversity [11]. Some papers [12, 13, 14] investigate the performance of a special form of the scheme when used for transmit antenna diversity. This special form is the most practical form of the scheme, which was also mentioned in the previous section. The signal is transmitted from the second antenna, then delayed one symbol period and transmitted from the first antenna. This scheme can be easily generalized to include M antennas at the base station and is often referred as delay diversity.

In [12], the performance of the delay diversity scheme is investigated for different numbers of transmit antennas using linear equalization, decision feedback equalization and maximum likelihood sequence estimation (MLSE) at the receiver and the results demonstrate the ability of the scheme to provide diversity benefit to a receiver in Rayleigh fading environment.

In [13], the diversity gain of the M-branch delay diversity scheme with maximum likelihood sequence estimation at the receiver is compared to M-branch receive diversity. The author concludes that delay diversity with M transmit antennas at the base station and single receive antenna at the mobile provides a diversity gain within 0.1 dB of that with single transmit antenna at the base station and M receive antennas at the mobile, for any number of antennas. Thus minimum distance reductions in the MLSE procedure do not introduce a significant degradation in the gain obtained by delay diversity.

In [14], the performance of a two-branch delay diversity scheme for the GSM system is obtained by simulations. For downlink, a delayed signal (in the order of two bit periods) is transmitted from a second antenna branch in order to introduce "artificial" time dispersion in the radio channel and the equalization capability of the GSM receiver is utilized. The results show that the two-branch scheme reduces the multi-path fading margin by 3-10 dB on the downlink for the GSM specified test channels.

There are also other interesting transmit diversity schemes, one of which is the famous Alomouti's scheme proposed in 1998 [15]. In [15], Alomouti proposes a simple two-branch spatial transmit diversity scheme which is different from delay diversity. Using two transmit antennas and one receive antenna the scheme provides the same diversity order as maximal receiver combining (MRRC) with one transmit antenna, and two receive antennas. The scheme does not require any bandwidth expansion and the correlation between signals from the two transmit antennas is such introduced that the computational complexity of the combining scheme at the receiver is similar to MRRC. However, the scheme cannot be generalized to M transmit antennas and consequently cannot be used for base station simulcasting. Also, the scheme is probably very sensitive to differential delays between the two paths, and the differential delays are inevitable in base station simulcasting case.

1.2   Scope of This Thesis

The papers reviewed in the previous section show that a transmit delay scheme can be used to provide diversity benefit to a receiver in a simulcast environment. The uncovered aspect related to transmit delay based simulcasting in these papers is that they give no idea about the coverage properties of the network. If a real simulcast network is to be implemented, the performance of the scheme at various mobile positions should be investigated. Depending on the mobile position, the relative delay of different paths and the relative power in these paths will differ. Obviously the performance of an equalizer employed at the receiver will depend on these two parameters. Therefore, the first step in investigating the coverage properties of the scheme should be the development of a model that will enable us to determine the power delay profile experienced by a receiver at different positions on the network.

Figure-4 illustrates a two basestation transmit delay scheme where a delay of one symbol period is introduced between the simulcasting base stations. The mobile is illustrated at a distance closer to the delayed base station. This is the location where the intentional delay introduced between base stations and the propagation delay difference between the two paths add up to zero. There is nothing that the equalizer

10
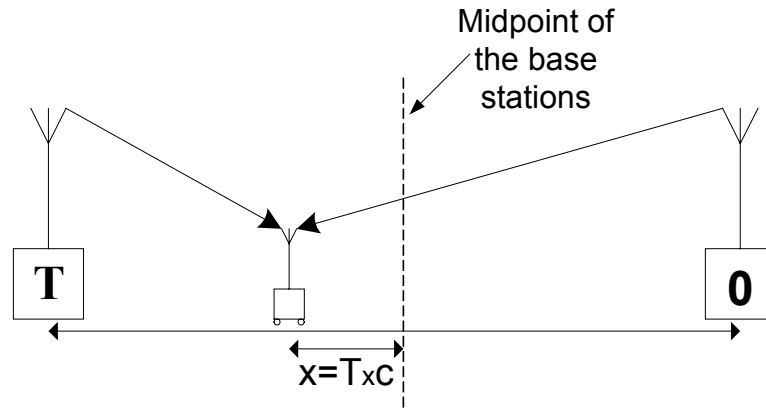
Figure-4 Two base station transmit delay scheme

can do at this point thus, no diversity gain is provided to the receiver. In such regions the performance may drop significantly below the average, resulting in coverage gaps on the service area. In [3], this case is pointed out as a serious disadvantage of the scheme.

The problem can be overcome by increasing the delay introduced between the base stations. However, increasing the delay will exponentially increase the computational complexity of the receiver. Thus, the delay to be introduced between the base stations arises as a critical parameter that should be optimized for optimum coverage. The dependency of optimum delay on network design parameters such as transmitter separation and SNR should also be investigated.

The papers overviewed in the previous sections are all interested in providing diversity gain to the receiver in Rayleigh fading environment. However, an important advantage of transmit delay based simulcasting comes to light when static propagation environment is considered. In the overlap areas the signals received from two static paths with a relative delay in the order of the RF carrier period will result in the spatial interference pattern illustrated in Figure-4. While discussing quasi-synchronous simulcasting we said that the pattern is still present in the overlap areas. Transmit delay based simulcasting extends the relative delays of the paths from different base stations in the overlap areas from the order of RF carrier period

to the order of symbol period. Thus, transforms the spatial interference pattern to ISI, which can obviously be handled with equalization.

In the context of this thesis we will carry out theoretical analysis and computer simulations to provide answers to the following questions:

- What are the coverage properties of a transmit delay based scheme in static and Rayleigh fading simulcast environments?
- What is the optimum delay to be introduced between base stations?
- What is the dependence of the optimum delay to network parameters like transmitter separation, SNR etc.?
- What is the performance of the scheme with MLSE?

    (Or equivalently, is there any performance degradation due to MLSE of interfered symbol stream compared to matched filter bound?)

The thesis is organized as follows. In Chapter 2, we will introduce our system model for transmit delay based simulcasting and derive the expression for received signal energy. The coverage properties of the scheme will be investigated based on this received signal energy expression, for two different channel models; the LOS channel and the Rayleigh fading channel in Chapter 3. The receiver models that can be employed in mobiles on a transmit delay based simulcast network are derived in Chapters 4 and 5 and the performance of these receiver models are investigated in Chapter 6.

CHAPTER 2

SYSTEM MODEL

In this chapter, we will introduce the simulcasting technique we suggest and develop a model for the radio channel experienced under the simulcasting scenario. The modeling process will be based on determining the energy of the composite signal received by the mobile station. The energy will be obtained as a function of receiver position, which will enable us to investigate the performance of the scheme at different mobile locations. In order to be able to carry out the theoretical analysis certain simplifications will be made but the model will still prove to be useful in the following chapters in evaluating the coverage properties of the scheme and quantifying the effect of such network design parameters such as delay introduced between base stations, transmitter separation and SNR.

In the last section of this chapter the technical features of the Pan-European PMR system TETRA will be briefly introduced since the simulations in the subsequent chapters will use TETRA parameters when required. Special emphasis will be placed on $\pi/4$-DQPSK, which is the modulation type in TETRA.

2.1   Introduction

The simulcasting technique we suggest is to introduce transmit delays between adjacent base stations on a network. The scheme is depicted in Figure-5 where the symbols in the middle of the cells denote the relative delay of the cell with respect to the center cell. In this figure a hexagonal cell configuration is assumed. The transmit delays are allocated such that the differential delay between signals received from two neighboring base stations is always different than zero in their overlap region.
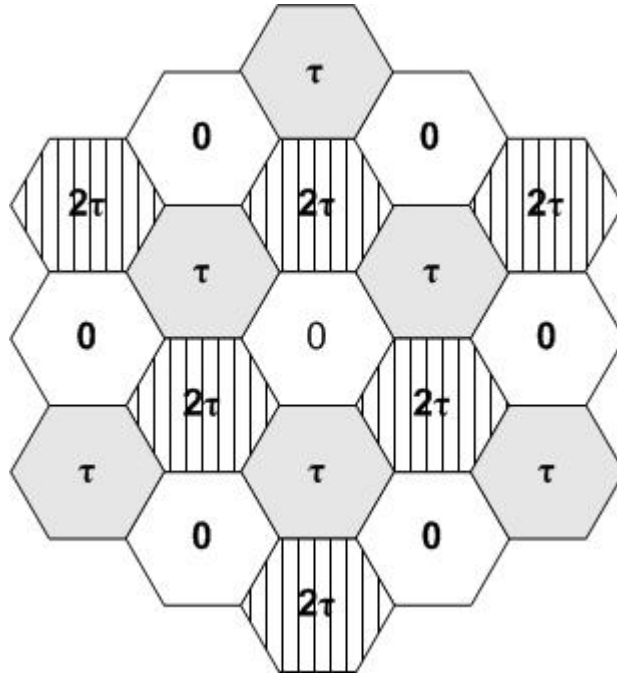
Figure-5 Transmit Delay Scheme for a Simulcast Network

2.2 System Model

In this section we will derive the energy of the composite signal received by the mobile station. Deriving an expression for the received energy when the mobile is located at any random position on the network in Figure-5 and considering the multipaths from all base stations is fairly complex. For the sake of simplicity, we will constrain our mobile station to move only along the axis connecting two neighboring base stations. Theoretical results will be derived considering only the signals received from these two base stations. This is a reasonable assumption because the received signal on this axis is dominated by the signals transmitted from these two nearest base stations.

Our simplified system model is shown in Figure-6 where one of the base stations is delayed by τ relative to the other, d is the base station separation and x is the

14

distance of the mobile to the middle of the base stations. The transmitted signals from the two base stations can be expressed as

$$s_1(t) = \text{Re}\{p(t)\exp(jw_ct)\}$$
$$s_2(t) = \text{Re}\{p(t-\tau)\exp(jw_ct)\}. \tag{1}$$

where $p(t)$ represents the baseband equivalent of the transmitted signal. The two waves originating from the two base stations will be attenuated according to the length of the path they travel before reaching the mobile station and in general one will have a relative delay due to the excess path it travels. Assuming that the individual channels between the base stations and the mobile are of slowly varying, flat fading nature, the received signal is

$$r(t) = \text{Re}\{(\alpha p(t) + \beta p(t - \tau - \tau_p))\exp(jw_ct + \phi)\} + n(t) \tag{2}$$

where α and β are the complex power scales of the respective channels and will be associated to mobile position by the end of this section. ϕ is the carrier phase. Since coherent demodulation will be assumed the complex baseband equivalent of the received signal is

$$r_l(t) = \alpha p(t) + \beta p(t - (\tau + \tau_p)) + z(t), \tag{3}$$

$n(t)$ being the real additive white Gaussian noise process with two-sided spectral density $N_0/2$ and $z(t)$ is the equivalent low-pass complex white noise process

$$z(t) = z_1(t) + jz_2(t)$$

each $z_i(t)$ being Gaussian, with spectral density N_0. While writing the low pass equivalent signal $r_l(t)$, we simply ignore the phase shift $\exp(j\phi)$ due to the carrier phase since we assume that α and β are complex variables in general. τ_p corresponds to the propagation delay difference between the two routes and can be expressed as

$$\tau_p = \frac{2x}{c} \tag{4}$$

15
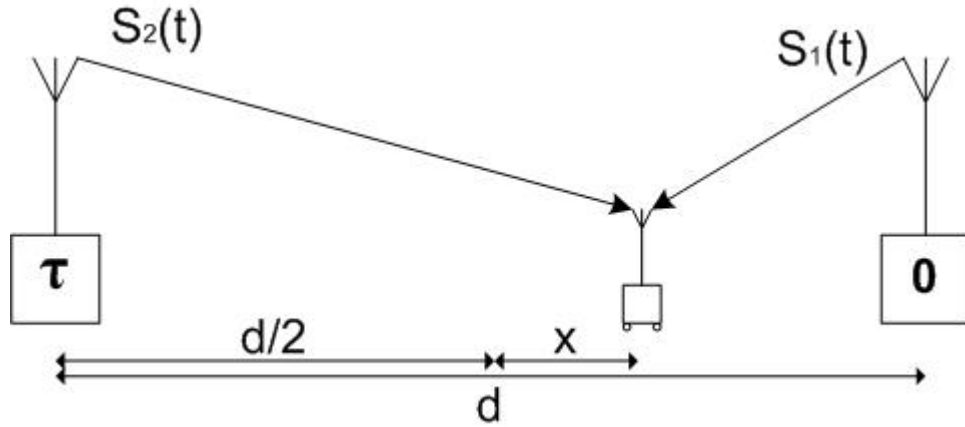
Figure-6 Two Base Station Transmit Delay Scheme

where $2x$ is the excess path traveled by the second ray with respect to the first and c is the speed of light. In the above notation x is the distance of the mobile from the mid point of the base stations and is positive if the mobile is close to the earlier base station.

Assuming linear modulation, the transmitted signal $p(t)$ appearing in Equations (2) and (3) has the general form,

$$p(t) = \sum_{n=0}^{\infty} S_n g(t - nT) \tag{5}$$

where $\{S_n\}$ represents the discrete information-bearing sequence of symbols and $g(t)$ is the basic pulse shape.

In general $p(t)$ transmitted through the two-path system above will suffer ISI, rendering both detection of the data symbols and the analysis more difficult. Regarding simplicity in the analysis, one can omit the effects of intersymbol interference (ISI) and find an estimate of the best performance (lower bound on the error rate) that can be expected from the system with uncoded data transmission by finding the performance based merely on the received symbol energy. Received

16

symbol energy is found by assuming that single symbol is transmitted through the system. Since the optimum detector of a single pulse is a matched filter, the bound obtained from single symbol transmission assumption (or sometimes referred as one shot transmission) is called the matched filter bound (MFB). MFB is one of the simplest quantities one can consider when assessing the capabilities of a noisy channel. Aside from providing an estimate of the best performance that can be expected from the system, it will provide insight on the parameters that determine the performance of the system in our case. In practice, the transmitted symbols will be determined by employing an equalizer at the receiver, a maximum likelihood sequence estimator (MLSE) in our case and obviously MLSE of the symbol stream may result in some performance loss compared to matched filter bound that is evaluated considering single symbol transmission [16]. The performance with continuous data transmission will be investigated in Chapter 4.

For single symbol transmission, $p(t)$ is a single real pulse, i.e. $g(t)$ of energy ε_g scaled by the complex symbol S_0. When, PSK or DPSK type modulation is considered, as we will consider in this thesis, $|S_n|^2 = 1$, for all n. Thus, without any loss of generality we will simply ignore S_0 in the following evaluations because it will not affect the received energy. The optimum demodulator from the point of view of signal detection is one matched to the received pulse

$$h(t) = \alpha g(t) + \beta g(t - (\tau + \tau_p)) \tag{6}$$

with impulse response $h^*(-t)$, assuming that the channel is known exactly. Here we assume quasi-static fading, that is, the coherence time of the channel is long enough that the impulse response may be considered to be constant over several symbol intervals. Thus, the slowly varying channel can be tracked and is thus known to the receiver. For quasi static fading a discrete time system description with one sample per symbol is possible at the matched filter output. With appropriate sampling of the matched filter output, the signal component of the sample value will be the energy in the received pulse. Thus,

$$\varepsilon = h(t) * h^*(-t)\,|_{t=0} = \int h(t) h^*(t) dt \,. \tag{7}$$

Performing the above integral, the energy in the received pulse evaluates to

$$\varepsilon = \varepsilon_g \left(|\alpha|^2 + |\beta|^2 + 2q(\tau + \tau_p)\,\mathrm{Re}\{\alpha\beta^*\} \right) \tag{8}$$

where $q(\eta)$ is the normalized autocorrelation function of $g(t)$, thus

$$q(\eta) = \frac{1}{\varepsilon_g} \int g(t) g^*(t-\eta) dt \,. \tag{9}$$

Note that ε is the energy in the baseband equivalent of the signal and the received energy in the bandpass signal is actually half of ε.

In order to derive the power delay profile experienced by the receiver we will assume a log distance propagation law model [17,18]. In the log-distance propagation model the average path loss for an arbitrary transmitter-receiver separation r is expressed as a function of distance by using a path loss exponent, in decibels [18],

$$PL(r) = PL(r_0) + 10\gamma \log_{10}\left(\frac{r}{r_0}\right) \tag{10}$$

where the path loss is defined as the difference between the effective transmitted and received powers, in decibels,

$$PL = -10\log_{10}\frac{P_{rec}}{p_{tr}} \,. \tag{11}$$

r_0 is the free space close-in reference distance and $PL(r_0)$ is the path loss to the reference distance r_0. $PL(r_0)$ is calculated using the free space path loss formula [18]. γ in Equation (10) is the path loss exponent that indicates the rate at which the path loss increases with distance. Typical path loss exponents obtained in various mobile environments are listed in Table-1.

The variation of the received power from a single base station can be expressed as a function of the mobile position x, using Equations (10) and (11) and taking the received power level at the middle of the base stations as a reference. Thus,

$$P_{rec1}(x) = P_{rec1}(x = 0) \left[\frac{(d/2)}{(d/2 - x)} \right]^{\gamma}$$

and

$$P_{rec2}(x) = P_{rec2}(x = 0) \left[\frac{(d/2)}{(d/2 + x)} \right]^{\gamma}.$$

(12)

where P_{rec1} and P_{rec2} are the powers in the signals received from the first and second base stations respectively. Assuming that the two transmitters at the two base stations are identical, and the channel properties are also identical, the path loss to the reference distance will be equal for both transmitters, thus $P_{rec1}(x = 0) = P_{rec2}(x = 0)$. The average power in the received rays is proportional to the second moment of the complex power scales α and β appearing in Equations (2) and (3). Thus, setting

$$E\left\{|\alpha|^2\right\}_{x=0} = E\left\{|\beta|^2\right\}_{x=0} = \frac{1}{2}$$

(13)

we obtain the following relations, that relate the second order statistics of α and β to mobile position x,

$$E\left\{|\alpha|^2\right\} = \frac{1}{2} \left[\frac{(d/2)}{(d/2 - x)} \right]^{\gamma}$$

(14)

$$E\left\{|\beta|^2\right\} = \frac{1}{2} \left[\frac{(d/2)}{(d/2 + x)} \right]^{\gamma}.$$

(15)

Table-1 Path Loss Exponents for Different Environments [18]

Environment	Path Loss Exponent, γ
Free space	2
Urban area cellular radio	2.7-4
Shadowed urban cellular radio	5-6
In building line of sight	1.6-1.8
Obstructed in building	4-6
Obstructed in factories	2-3

2.3 TErrestrial Trunked RAdio, TETRA

TETRA is the new Pan European standard for digital private mobile radio, prepared by ETSI (European Telecommunications Standardization Institute). The standard is applicable to private systems, such as security and emergency, field services, utilities etc. TETRA standard is defined to support both voice and digital services (V+D), and offers far more enhanced features compared to existing analog standards. The simulations in the following chapters are based on TETRA parameters. Hence a brief overview of the technical properties of the standard is given in the following paragraphs.

The system uses a frequency division multiple access (FDMA) structure with 25-kHz RF Channels both in the uplink and downlink directions. Each RF channel implements a time-division multiple access (TDMA) structure supporting four logical levels (for voice, data or signaling). The modulation scheme is π/4-shifted differential quaternary phase shift keying (π/4-DQPSK) with root-raised cosine modulation filter and a roll-off factor of 0.35. The basic radio resource is a timeslot lasting 14.167 ms transmitting information at a modulation rate of 36 kbit/s, or 18 kS/s. This means that the time slot duration, including guard and ramping times is 510 bit (255 symbol) durations. After deducting the overheads, each channel can

support a data rate of 7.2 kb/s. Also several TDMA slots can be combined to give a total data rate of 28.8 kb/s. The requirements specified in [19] are valid for systems operating in the range of 300 MHz to 1 GHz.

The basic TETRA parameters are summarized in Table-2. Detailed information about the modulation filter is given in Appendix-A and the modulation type is investigated in detail in the following subsection.

Table-2 TETRA Parameters

Access Scheme	4 slot TDMA
Channel Spacing	25 kHz
Frequency Band	300Mhz-1 GHz
Modulation	π/4-DQPSK
Modulation Filter	Root Raised Cosine with roll-off factor 0.35
Carrier Symbol Rate	18 kS/s
User Data Rate	7.2 kb/s per time slot

2.3.1 π/4-DQPSK

π/4 DQPSK is widely used in digital cellular communication systems such as IS-54 and the Japanese JDC. The scheme is also employed in TETRA and is defined in the TETRA standard [19] as follows.

Let $B(m)$ denote the information bit of a sequence to be transmitted, where m is the bit number. The sequence of information bits shall be mapped onto a sequence of modulation symbols $S(k)$, where k is the corresponding symbol number. The

modulation symbol *S(k)* shall result from a differential encoding. This means that *S(k)* shall be obtained by applying a phase transition *Dϕ(k)* to the previous modulation symbol *S(k-1)*, hence, in complex notation:

$$S(k) = S(k-1)\exp(jD\phi(k))$$
$$S(0) = 1 \tag{16}$$

The above expression for *S(k)* corresponds to the continuous transmission of modulation symbols. The symbol *S(0)* is the symbol before the first symbol of a continuous transmission and is transmitted as a phase reference.

The phase transition *Dϕ(k)* is related to the information bits as shown in Table-3 and Figure-7. Gray code is used in the mapping in Table-3; thus, the adjacent symbols differ in a single bit. Since the most probable errors due to noise result in the erroneous selection of an adjacent phase to the true phase, most two-bit symbol errors will contain only a single bit error.

Table-3 Phase Transitions in π/4 DQPSK

B(2k-1)	B(2k)	Dϕ(k)
1	1	-3π/4
0	1	+3π/4
0	0	+π/4
1	0	-π/4
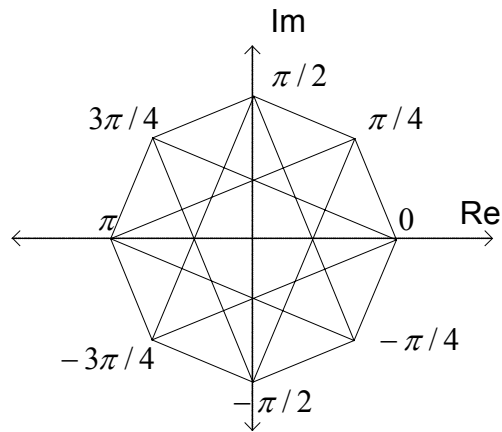
Figure-7 Phase Transitions in π/4 DQPSK

The complex symbol S(k) shall take one of the eight values $\exp(jn\pi/4)$, where $n=2, 4, 6, 8$ for even k and $n=1, 3, 5, 7$ for odd k. Figure-8 shows modulation symbol constellations for odd and even values of k. Although differential detection of π/4 DQPSK is more popular in general, in this thesis we will assume coherent demodulation of the signal, so that we can employ equalization after demodulation.
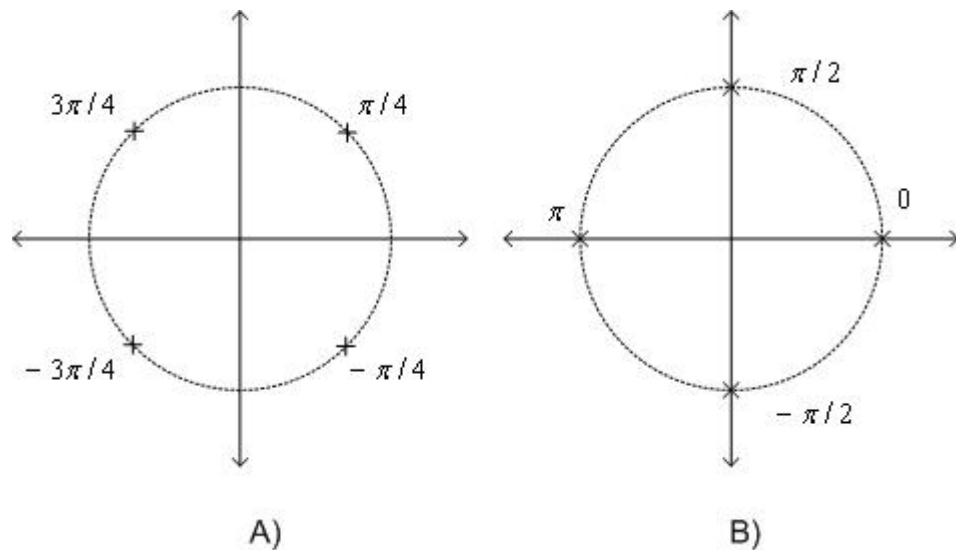
Figure-8 Modulation Symbol Constellations for A) Odd and B) Even Values of k

The received signal is demodulated and detected to one of the 4 possible transmitted symbols in either A or B in Figure-8, depending on the signaling interval. We observe that the symbol constellations in Figure-8 are not different from the signal constellation of QPSK. Because the probability of error is determined by the distances between pairs of symbol points, when coherent demodulation is assumed the probability of error for coherently detected $\pi/4$ DQPSK should not be different from the error probability for QPSK except for a factor that comes because in $\pi/4$ DQPSK the information is encoded in the differential phase and not in the absolute phase of the symbol. With differential encoding, an error in the demodulated phase of the signal in any given interval will usually result in decoding errors of the differential phase over two consecutive signaling intervals, that is with the Gray encoding given in Table-3 a single symbol error will usually result in two bit errors. This is especially the case for error probabilities below 0.1 [21]. Therefore, the probability of error for coherent demodulation of $\pi/4$ DQPSK is approximately twice the probability of error for QPSK with absolute phase encoding. However, this-factor-of-2 increase in the error probability translates into a relatively small loss in SNR. Thus, the bit error probability for QPSK is given in [21, p.268] as,

$$P_b = Q\left(\sqrt{\frac{2\varepsilon_b}{N_0}}\right) \tag{17}$$

and based on the above discussion, the bit error probability for coherently detected $\pi/4$ DQPSK is

$$P_b = 2Q\left(\sqrt{\frac{2\varepsilon_b}{N_0}}\right) \tag{18}$$

where ε_b is energy per bit and is half the energy per symbol for quaternary signaling. The energy per symbol is half of the energy in the baseband equivalent signal (8). Thus,

$$\varepsilon_b = \frac{\varepsilon_s}{2} = \frac{\varepsilon}{4}. \tag{19}$$

And

$$P_b = 2Q\left(\sqrt{\frac{\varepsilon}{2N_0}}\right) \tag{20}$$

where ε is derived in (8).

The basic advantage with π/4 DQPSK is the spectral efficiency. QPSK, due to the instantaneous π phase shift, leads to a significant spectral regrowth and thus has a low spectral efficiency. In a π/4 DQPSK system, the instantaneous phase transitions are limited to $\pm \frac{3\pi}{2}$, thus the spectral regrowth is reduced. In this manner, π/4 DQPSK is more advantageous compared to QPSK and is widely preferred in wireless communications for this advantage.

CHAPTER 3

PERFORMANCE EVALUATION BASED ON RECEIVED ENERGY

In this chapter we will evaluate the performance of the transmit delay scheme for two different channel models, based on the theoretical results from the previous chapter. By channel model we here refer to the channel model between a single base station and the mobile terminal. The overall channel model with simulcasting and the energy of the composite signal have been derived in the previous chapter, based on the assumption that the individual channels between the base stations and the mobile terminal do not introduce distortion on the signals originating from these base stations. The distortion on the received signal is due only to the multipath nature of the simulcast environment. Thus, in the previous chapter we associated a gain and phase shift to the individual channels, but we did not say anything about the nature of these channel parameters.

In this chapter we will assume two different models for the nature of the gain of the channel, thus two different channel models between the base stations and the mobile terminal. These two channel models are the additive white Gaussian noise (AWGN) channel which corresponds to a line of sight (LOS) condition between a transmitter and a receiver with essentially no multipath, and the Rayleigh fading channel which occurs when there is no direct path (LOS) between a transmitter and a receiver and the received signal is a sum of many reflected waves from the surrounding environment. These two channel models are chosen to illustrate the ability of the scheme to cancel the spatial interference pattern due to artificial multipath in simulcasting and providing diversity benefit to the receiver.

3.1 The LOS Channel

The LOS channel is the simplest type of channel that occurs when we have strong direct path between the transmitter and the receiver. It is often referred to as the additive white Gaussian noise (AWGN) channel since it corrupts the transmitted signal only by the addition of white Gaussian noise. Basically, the noise is the one generated in the receiver. The noise is assumed to be Gaussian, having a constant power spectral density over the channel bandwidth.

The AWGN channel is not often the case in digital mobile radio, but is also not improbable. Even when there is multipath fading, but the mobile is stationary and there are no moving objects in its vicinity, the mobile channel may be thought of as Gaussian with the effects of fading represented by a local path loss (see Table-1) The AWGN channel is also important for providing an upper bound on system performance [22].

3.2 Performance of the Scheme with LOS Channels

For LOS propagation from both base stations, the channel for a given mobile position x, is fixed. Thus, the magnitudes of the power scales α and β in (14) and (15) will be deterministic,

$$|\alpha|^2 = E\{|\alpha|^2\} = \frac{1}{2}\left[\frac{(d/2)}{(d/2-x)}\right]^\gamma$$

$$|\beta|^2 = E\{|\beta|^2\} = \frac{1}{2}\left[\frac{(d/2)}{(d/2+x)}\right]^\gamma. \tag{21}$$

The phases of α and β will change by 2π when the mobile changes position in the order of the carrier wavelength. When the carrier frequency is assumed to be 400 MHz, this corresponds to a distance less than a meter (λ_c= 0.75 m). Thus, phases of α and β may well be approximated by uniformly distributed statistically independent random variables over the network.

Illustration 1

Let us remember the expression derived in the previous chapter for the energy of the composite signal as (8)

$$\varepsilon = \varepsilon_g \left(|\alpha|^2 + |\beta|^2 + 2q(\tau + \tau_p) \operatorname{Re}\{\alpha\beta^*\} \right). \tag{22}$$

In this expression $q(\eta)$ is the normalized autocorrelation function of $g(t)$. In the rest of this thesis, without any loss of generality, we will assume that $g(t)$ is the ideal symbol waveform, obtained by the inverse Fourier transform of a square root raised cosine spectrum, in which case $q(\eta)$ has the raised cosine spectrum and is depicted in Figure-9.
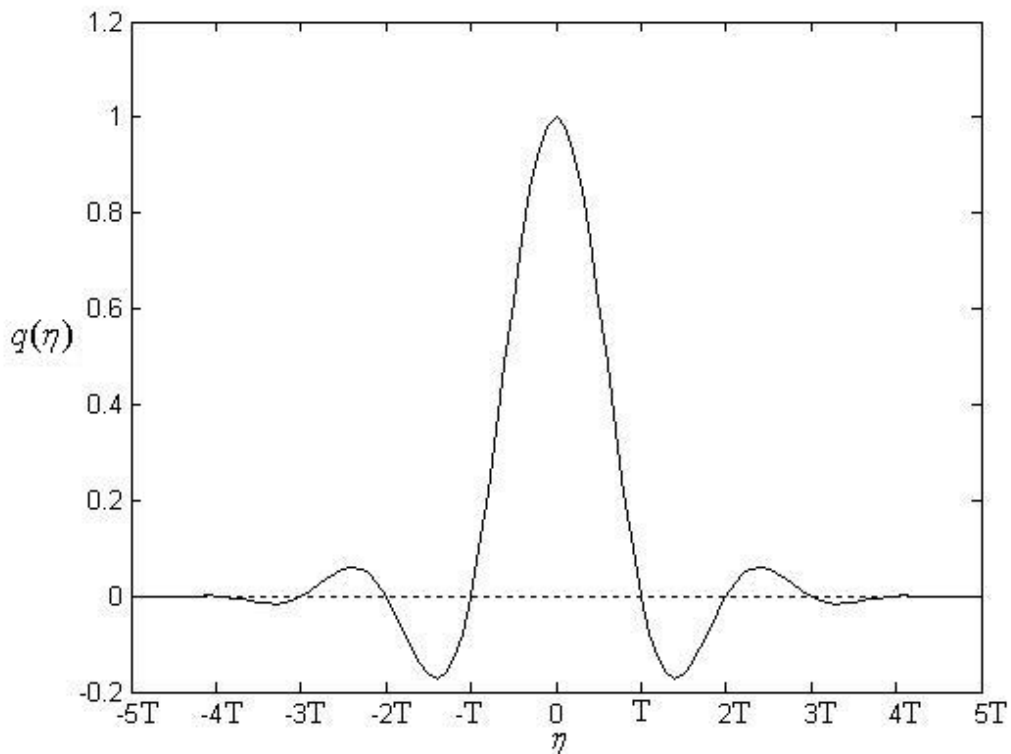
Figure-9 Raised Cosine Spectrum Pulse, Roll of Factor = 0.35

T is the symbol period.

Let us investigate the energy expression in (22) and try to develop an opinion about the coverage properties of the transmit delay scheme. Note that $q(\eta)$ takes its maximum value when $\eta = 0$, thus $q(\tau + \tau_p) = q(0) = 1$. In this situation, if α and β are of approximately equal magnitude and opposite phases (that is, $\angle\alpha = \theta$ and $\angle\beta = \pi + \theta$), the terms in the energy expression in (22) may add up to a small value, resulting in a deep fade. This is the case when we have a mobile terminal in the overlap zone of two base stations and, the base stations are transmitting simultaneously with no transmit delay strategy. Thus, $\tau_p \cong \tau = 0$. In the overlap zone, it is likely that the signals from the two base stations arrive at comparable power levels; therefore, deep fades may be experienced by the mobile terminal, depending on the phase difference between the RF carriers. The deep fades will tend to disappear when the mobile moves towards one of the base stations, basically because of two reasons. The mobile terminal, will now receive a stronger signal form the nearby base station and a weaker signal from the farther one, the difference between the power levels of the signals diminishing the effect of destructive interference. The second and more important effect is that, the coefficient $q(\tau + \tau_p)$ of the interference term in the energy expression in (22) decreases with increasing propagation delay difference τ_p (Note that $\tau = 0$ for the present case). When the propagation delay difference between the two waves is equal to the symbol period, the interference term totally disappears (see Figure-9, $q(T) = q(-T) = 0$); the multipath interference is now resolved to provide diversity gain to the receiver.

From Figure-9, we may expect the deep fades to be effective in a region where the propagation delay difference between the two paths is less than half of the symbol period, because the interference term is still significant in this region ($q\left(\dfrac{T}{2}\right) = q\left(-\dfrac{T}{2}\right) = 0.6186$). Remembering Equation (4) for the propagation delay difference, this corresponds to a region 8.33 km wide around the mid point of the base stations, when a symbol rate of 18 kS/s is assumed.

When transmit delay is introduced between the two base stations, we may still expect to observe fades in the region where the intentionally introduced delay between the base stations and the propagation delay add up to zero. This region will be located closer to the delayed base station and the effect of the fades will weaken as the region approaches closer and closer to the base station. ☐

This discussion was to illustrate the idea that with the transmit delay scheme, we expect to have coverage property that possesses coverage gaps in certain regions. These coverage gaps are the regions where the performance of the scheme drops significantly below the average. In the rest of this chapter our aim will be to overcome the problem of coverage gaps, by adjusting different network parameters.

In the literature, coverage results have been presented in different ways; a continuous coverage plot over the service area, calculation of outage probability or a bit error rate (BER) distribution over the service area [1, 23]. For our problem, we would like our coverage measure to enable us quantify the effect of coverage gaps inherent in the network as a function of different network design parameters. Using the worst value of the performance criteria over the network as a coverage measure is convenient for our purpose and can be used to identify the coverage properties of a transmit delay scheme. In the rest of this thesis, we will use the worst performance value on the simulcast network as a coverage measure of the scheme. To find the worst performance value, we will evaluate the performance of the scheme at sufficiently many different mobile locations on the network and choose the worst one. Remembering the above illustration, this worst performance does not correspond to a single isolated failure event but indicates poor coverage over a certain region.

Returning to the energy expression in (22), the energy ε in the received pulse satisfies the following inequality

$$\varepsilon \geq \varepsilon_g \left(|\alpha|^2 + |\beta|^2 - abs(2q(\tau + \tau_p)|\alpha\|\beta|) \right) \tag{23}$$

where for a given mobile position x, $|\alpha|$ and $|\beta|$ are determined by the equations in (21) and τ_p is determined by Equation (4). In the inequality, $abs(.)$ refers to the absolute value of $(.)$ and the expression in absolute value parentheses is the maximum possible value for the interference term, at a given mobile location.
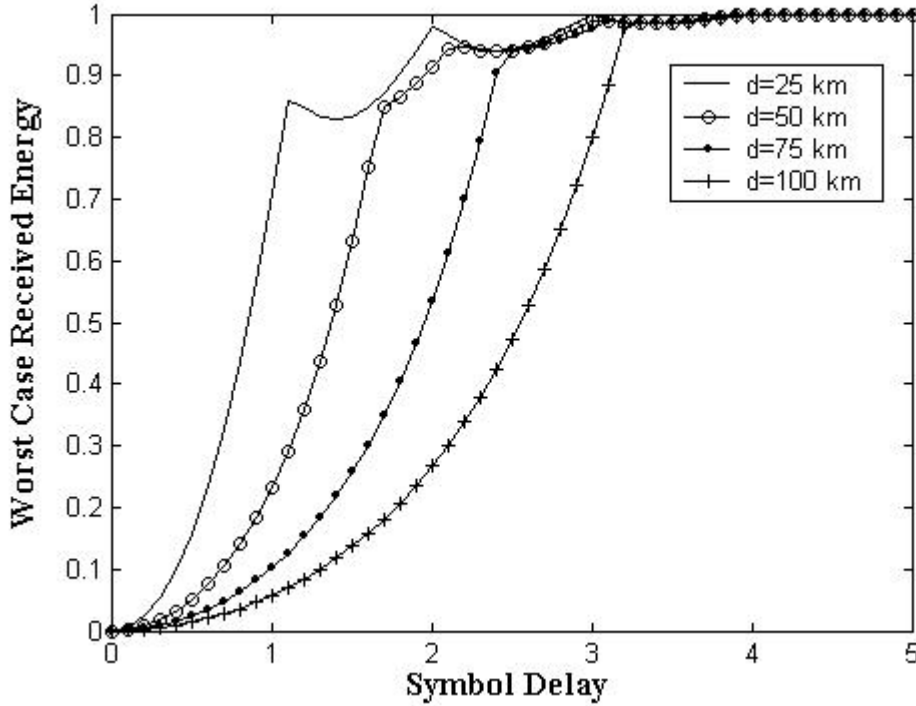
Figure-10 Worst case received energy versus delay introduced between base stations for LOS channel model

Figure-10 depicts the worst case received energy on the simulcast network as a function of the delay introduced between base stations, taking base station separation as a parameter. $g(t)$ has a square-root-of raised-cosine spectrum with roll off factor of 0.35. Symbol rate is equal to 18 kS/s and γ is 2. From Figure-10, we observe that by introducing a transmit delay of two symbol periods between 50 km separated two base stations, the minimum received energy on the network increases from 0 to 0.9, resolving the multipath interference due to simulcasting and additionally providing

diversity gain to the receiver. The optimum delay to be introduced between base stations increases with increasing base station separation.

Since the channel for a given mobile position is fixed with LOS propagation, the worst case probability of errors, corresponding to the worst case received energies in Figure-10 are simply a particular function (the co-error function) of the ratio of the received pulse energy to noise spectral density (SNR). The exact relation between received energy and bit error probability is given in Equation (20) for $\pi/4$ shifted DQPSK.

3.3   The Rayleigh Fading Channel

In mobile radio systems, there are usually several transmission paths from the base station to the mobile, due to reflections and diffractions form surrounding buildings, cars or other urban paraphernalia. This phenomenon is referred as multipath propagation and is basis for the special problems associated to wireless communication. Multipath propagation causes short-term fluctuations in received signal energy that is called small-scale fading to distinguish it from the large-scale variation in mean signal level, which is dependent on transmitter-receiver separation discussed in the previous chapter. Small-scale fading is caused by wave interference between two or more multipath components that arrive at the receiver while the mobile travels a short distance (a few wavelengths) or over short period of time. These waves combine vectorally at the receiver antenna to give the resultant signal, which can vary widely in amplitude, depending on the distribution of phases of the waves and the bandwidth of the transmitted signal.

Small scale fading is generally classified as being either flat or frequency selective. If the mobile radio channel has a constant gain and a linear phase response over a bandwidth that is greater than the bandwidth of the transmitted signal, then the received signal will undergo flat fading. This occurs when all the multipath components manifest themselves in a bunch with negligible delay spread between them. This type of fading does not introduce time distortion (no inter symbol interference) on the transmitted signal. The strength of the received signal, however,

will change with time, due to fluctuations in the gain of the channel caused by multipath.

When there are a large number of paths, it is reasonable to regard the unpredictable amplitudes and phases of the interfering paths being random. It is also reasonable to assume that the phases and amplitudes of different rays are statistically independent. Based on these assumptions, the central limit theorem may be applied to yield a time varying channel impulse response that can be modeled as a complex valued zero-mean Gaussian random process. This model has proven to give good prediction of measured signal statistics; therefore it has become widely accepted. A further reasonable assumption is that the fading process is wide sense stationary, in fact strictly stationary, since it is Gaussian.

Thus assuming flat fading, the multiplicative distortion introduced by the channel at any time instant is a zero-mean complex Gaussian random variable. As a consequence, the phase of the channel gain is a uniformly distributed random variable and the amplitude has Rayleigh distribution, hence comes the name Rayleigh fading.

3.4   Performance of the Scheme in Rayleigh Fading Environment

In this section we will investigate the performance over a transmit delay based network in flat Rayleigh fading environment. Assuming flat Rayleigh fading channels from both base stations to the mobile terminal, the power scales $\alpha(t)$ and $\beta(t)$ at a given mobile position are statistically independent, identically distributed zero-mean complex Gaussian processes, the second order statistics of the stationary processes determined by large-scale variations.

In the derivations of the previous chapter, we assumed quasi static fading, that is, the channel can be tracked and is thus, known. At a particular time, α and β are zero-mean complex Gaussian random variables such that (14) (15)

33

$$E\{\alpha_R{}^2\} = E\{\alpha_I{}^2\} = E\{|\alpha|^2\} = \frac{1}{2}\left[\frac{(d/2)}{(d/2-x)}\right]^{\gamma} = p_{\alpha}$$

$$E\{\beta_R{}^2\} = E\{\beta_I{}^2\} = E\{|\beta|^2\} = \frac{1}{2}\left[\frac{(d/2)}{(d/2+x)}\right]^{\gamma} = p_{\beta} \tag{24}$$

where α_R, α_I, β_R, β_I denote the real and imaginary parts of α and β respectively.

Illustration 2

In Illustration 1 we have illustrated how the transmit delay scheme acts to solve the multipath interference problem in simulcasting with LOS propagation. In this part we would like to illustrate how the scheme can be used to provide diversity benefit to the receiver by again elaborating the energy expression in (22). Let us recall the expression for received energy, derived in the previous chapter:

$$\varepsilon = \varepsilon_g \left(|\alpha|^2 + |\beta|^2 + 2q(\tau + \tau_p)\operatorname{Re}\{\alpha\beta^*\}\right). \tag{25}$$

We will again start with the case when no transmit delay strategy is employed between base stations, $\tau = 0$, and considering the overlap area of two base stations where $\tau_p \cong 0$. Therefore, $q(\tau + \tau_p) \cong 1$ in this region. Based on this assumption we can rewrite the energy expression in the following simple form

$$\varepsilon = \varepsilon_g |\alpha + \beta|^2. \tag{26}$$

Let us also consider the case when transmit delay strategy is employed and a delay of one symbol period is introduced between base stations, hence $\tau = T$. Considering again the overlap zone of two base stations we may assume that the propagation delay difference between two paths is approximately zero, $\tau_p \cong 0$, hence $q(\tau + \tau_p) \cong q(T) = 0$. This assumption leads to the following simplified expression for received energy

$$\varepsilon = \varepsilon_g (|\alpha|^2 + |\beta|^2). \tag{27}$$

Comparing the energy expressions in (26) and (27), we see that in the first case the mobile station observes the sum of the fading variables α and β which may add up either constructively or destructively. When transmit delay strategy is employed the individual paths are distinguished by the mobile terminal and the individual contributions always add up constructively. A diversity gain of order two is obtained because the probability that both fading variables are small is much smaller than the probability that a single fading variable α or β is small. □

In the previous section we used received energy as a performance criteria for LOS channels. In that situation, the received energy was deterministic for a given mobile position and was directly related to the probability of error. For an ensemble of channels such as experienced as a time sequence with small-scale fading, the received energy at a given mobile position is a random variable. Thus, the mean bit error probability is dependent on received energy probability density function (PDF) and will be used directly as the performance criteria for Rayleigh fading environment.

The probability of bit error for $\pi/4$ DQPSK was given in Equation (20). When the received energy ε in the equation is a random variable, resulting from an ensemble of channels, the complementary error function must be averaged over all possible channels, hence

$$P_b = 2E\left\{Q(\sqrt{\frac{\varepsilon}{2N_0}})\right\}. \tag{28}$$

The expectation is evaluated in [16] to find the mean bit error probability for 2 or 4 PSK considering two-beam Rayleigh fading. Starting with the bit error probability expression for $\pi/4$ DQPSK we will follow the procedure in [16] and use the results of the mathematical derivations to find a closed form expression for P_b with $\pi/4$ DQPSK in transmit delay scheme based simulcast environment.

Let us start with rewriting the expression for P_b explicitly using the complementary error function,

$$P_b = 2E\left\{\frac{1}{2}erfc(\sqrt{\frac{\varepsilon}{4N_0}})\right\} \tag{29}$$

and recall that the complementary error function is defined as

$$erfc(x) = \frac{2}{\sqrt{\pi}}\int_x^\infty \exp(-t^2)dt = 1 - \frac{2}{\sqrt{\pi}}\int_0^x \exp(-t^2)dt . \tag{30}$$

Writing P_b in detail,

$$P_b = 1 - \frac{2}{\sqrt{\pi}}E\left\{\int_0^{\sqrt{Q}} \exp(-t^2)dt\right\} = 1 - \frac{2}{\sqrt{\pi}}\int_0^\infty p(Q)dQ \int_0^{\sqrt{Q}} \exp(-t^2)dt \tag{31}$$

where

$$Q = \frac{\varepsilon}{4N_0} = \frac{\varepsilon_g}{4N_0}\left(|\alpha|^2 + |\beta|^2 + 2q(\tau + \tau_p)\text{Re}\{\alpha\beta^*\}\right). \tag{32}$$

and $p(Q)$ denoting the probability density function of $Q \geq 0$. $p(Q)$ can be found from the inverse Fourier transform of the characteristic function $\psi_Q(j\omega)$, thus

$$p(Q) = \frac{1}{2\pi}\int_0^\infty \psi_Q(j\omega)\exp(-j\omega Q)d\omega . \tag{33}$$

Q is a quadratic form in fading variables α and β. The characteristic function for a quadratic form of Gaussian random variables is well known [21] and in Appendix-2, it is shown that for our problem

$$\psi_Q(j\omega) = \frac{1}{(1 - j\omega\rho d_1)(1 - j\omega\rho d_2)} \tag{34}$$

where

$$d_{1,2} = \frac{\left(p_\alpha + p_\beta\right) \mp \sqrt{\left(p_\alpha - p_\beta\right)^2 + 4 p_\alpha p_\beta q^2 \left(\tau + \tau_p\right)}}{2} \tag{35}$$

and

$$\rho = \frac{\varepsilon_g}{2 N_0}. \tag{36}$$

The integrals in (31) are performed in [16]. Using the result in [16] yields the following expression for P_b,

$$P_b = \left[1 - \frac{1}{d_1 - d_2} \left(\frac{\sqrt{\rho d_1}}{\sqrt{\rho + \frac{1}{d_1}}} - \frac{\sqrt{\rho d_2}}{\sqrt{\rho + \frac{1}{d_2}}} \right) \right], \text{ when } d_1 \neq d_2 \tag{37}$$

and

$$P_b = \left[1 - \left(\frac{\sqrt{\rho}}{\sqrt{2 + \rho}} - \frac{\sqrt{\rho}}{\left(\sqrt{2 + \rho}\right)^3} \right) \right], \text{ when } d_1 = d_2 = p_\alpha = p_\beta \tag{38}$$

where d_1, d_2 and ρ are defined in (35) and (36) respectively.
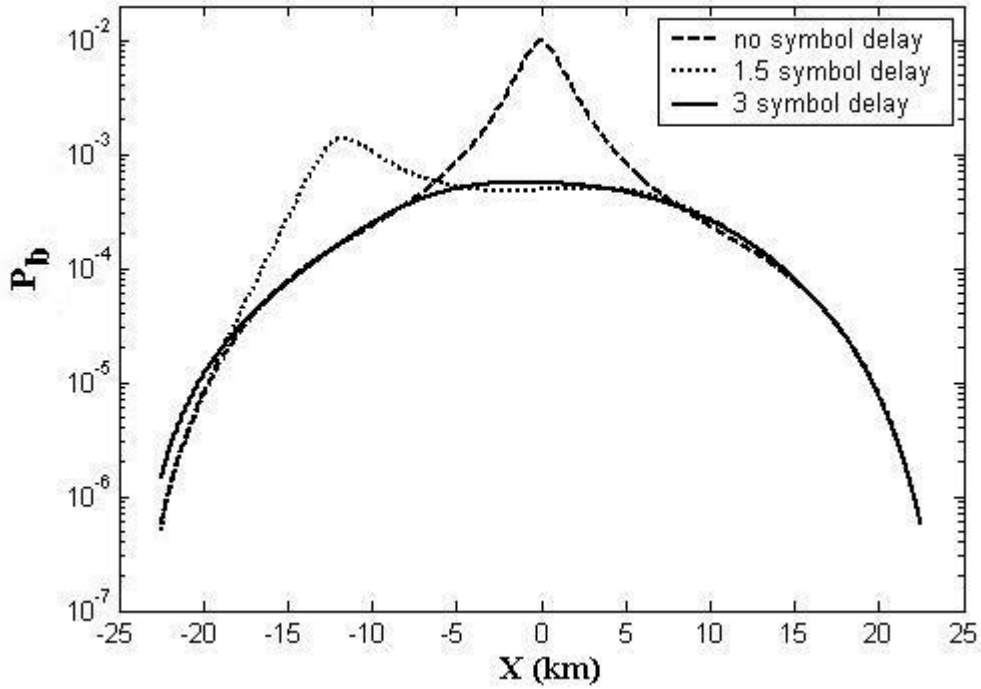
Figure-11 P_b variation over the simulcast network for $d = 50km$

In Figure-11, we observe the variation of P_b along the axis connecting two 50 km separated base stations when the base stations transmit simultaneously with no transmit delay strategy and when a delay of 1.5 and 3 symbol periods is introduced between base stations. We have used $\gamma = 4$, which is reasonable for urban area cellular radio (Table-1) and $\rho = 50$. This ρ value corresponds to an averaged received SNR per symbol of 17 dB when the mobile is at the midpoint of the base stations. From Figure-11 we observe the phenomena of coverage gaps on a transmit delay based network, discussed in the previous sections for LOS propagation. By introducing transmit delay between the base stations, the coverage gaps shift from the middle of the base stations to the delayed base station, meanwhile weakening in effect. When a transmit delay of 3 symbol periods is introduced between base stations we have a smooth performance over the network with no coverage gaps.

Figure-12 shows the worst P_b on the network as a function of the delay introduced between base stations for different base station separations. Figure-13 depicts the variation of worst P_b with ρ, the delay introduced between 50 km separated base stations being a parameter. The worst P_b values in these figures correspond to the peak values in Figure-11. Figure-12 and Figure-13 imply that for a given base station separation and SNR the improvement in performance that can be achieved by increasing the delay is lower bounded. Increasing the delay further than the optimum delay value increases receiver complexity but no more improvement in worst P_b is achieved. As an example, for base station separation of 50 km and $\rho = 17\,\text{dB}$, a tranmit delay of 1.85 symbol periods is sufficient. There is no need to increase the delay further because this will not improve the performance over the network.
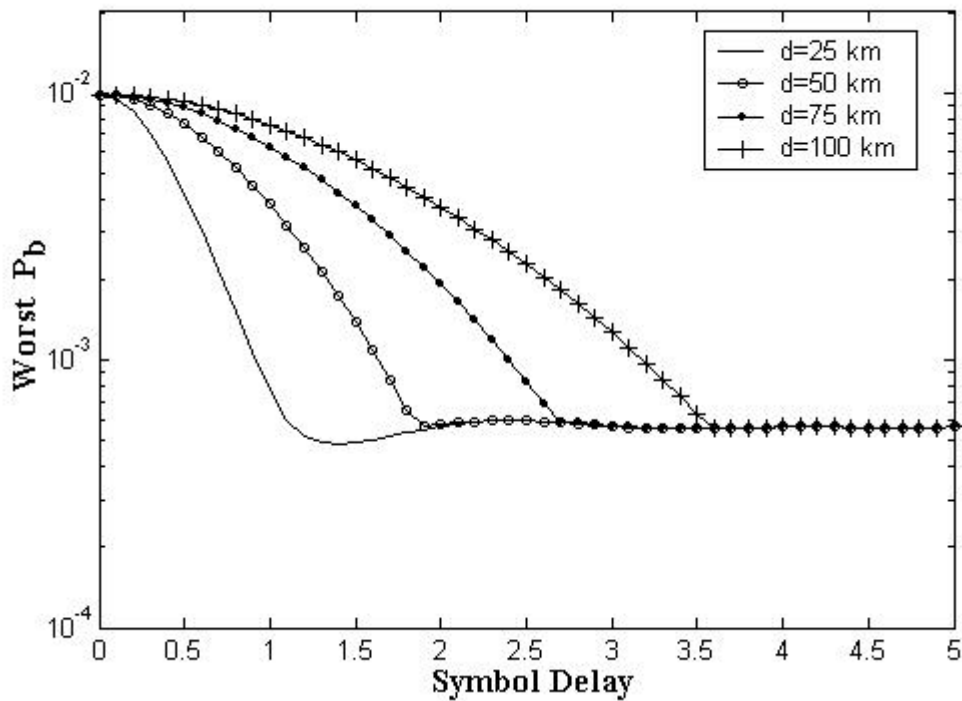
Figure-12 Worst P_b versus delay introduced between base stations in

Rayleigh fading environment
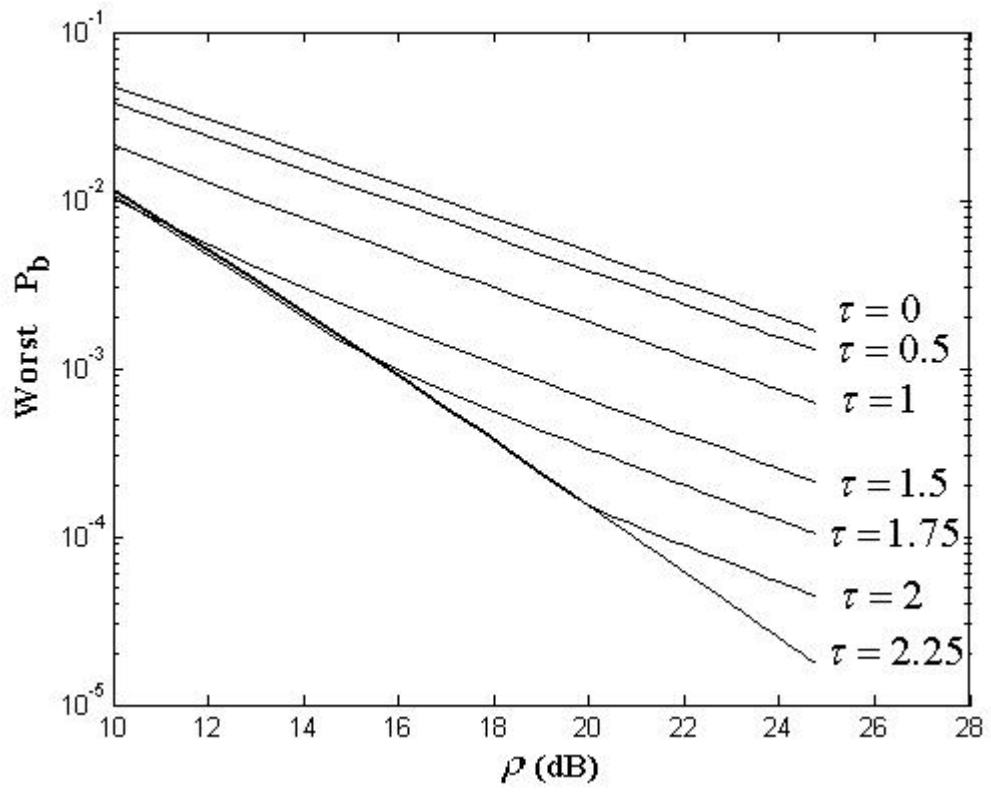
Figure-13 Worst P_b versus SNR for different τ values

CHAPTER 4

RECEIVER MODELS

In the previous chapter, we evaluated the performance of the scheme based on received symbol energy. While deriving the expression for received symbol energy we thought as if a single symbol were transmitted through the system. This is a hypothetical situation that does not occur in practice. In practice, the transmit delay scheme will be used to transmit continuous data and the multipath nature of the simulcast network will cause ISI. In order to remove the ISI channel equalizers should be employed at the receivers. In this and the following chapters we will assume a maximum likelihood sequence estimator (MLSE) at the receiver.

Before the maximum likelihood sequence estimator acts the time continuous received signal must be discretized. The discretization is to be done by the demodulator. In the receiver we will employ two different demodulators, an optimum demodulator that together with the maximum likelihood sequence estimator forms an optimum maximum likelihood receiver for channels with ISI and a suboptimum but simplified demodulator. In this chapter we will introduce the demodulators and derive the corresponding discrete time channel models. Based on these channel models, the performance of the maximum likelihood sequence estimator will be derived in the following chapter.

4.1   Whitened Matched Filter

The low pass equivalent of the signal received by a mobile terminal on a transmit delay based simulcast network is given by Equation (3) as

$$r_l(t) = \alpha p(t) + \beta p(t - (\tau + \tau_p)) + z(t) \qquad (39)$$

where $p(t)$ is the low pass equivalent transmitted signal that has the common form in (5) with different types of digital linear modulation techniques including $\pi/4$ shift DQPSK and $z(t)$ represents the additive white Gaussian noise with variance N_0. Here we continue with the quasi static fading assumption. The received signal can be equivalently represented as,

$$r_l(t) = \sum_{n=0}^{\infty} S_n h(t - nT) + z(t) \qquad (40)$$

where

$$h(t) = \alpha g(t) + \beta g(t - (\tau + \tau_p)) \qquad (41)$$

represents the response of the channel to the input signal pulse $g(t)$.

Following the approach in [21], let us express the received signal $r_l(t)$ in its series expansion over a complete set of orthonormal functions $\{f_k(t)\}$ as,

$$r_l(t) = \lim_{N \to \infty} \sum_{k=1}^{N} r_k f_k(t) \qquad (42)$$

where $\{r_k\}$ are the coefficients obtained by projecting $r_l(t)$ onto each of the functions $\{f_k(t)\}$. By using the Equation (40), one may show that the coefficient r_k, resulting from projecting $r_l(t)$ onto $f_k(t)$ may be expressed as

$$r_k = \sum_{n} S_n h_{kn} + z_k \qquad k = 1,2,\dots \qquad (43)$$

where h_{kn} and z_k are the values obtained from projecting $h(t - nT)$ and $z(t)$ onto $f_k(t)$, respectively. The sequence $\{z_k\}$ is Gaussian distributed with zero mean and covariance

$$\frac{1}{2}E(z_k^* z_m) = N_0 \delta_{km} . \tag{44}$$

Hence, the coefficients $\{r_k\}$ are also Gaussian distributed independent random variables. Thus, the joint probability density function of the random variables $\mathbf{r}_N \equiv \begin{bmatrix} r_1 & r_2 & \cdots & r_N \end{bmatrix}$ conditioned on the transmitted sequence $\mathbf{S}_p \equiv \begin{bmatrix} S_1 & S_2 & \cdots & S_p \end{bmatrix}$, where $p \leq N$, is

$$p(\mathbf{r}_N \mid \mathbf{S}_p) = \left(\frac{1}{2\pi N_0} \right)^N \exp\left(-\frac{1}{2N_0} \sum_{k=1}^{N} \left| r_k - \sum_n S_n h_{kn} \right|^2 \right) \tag{45}$$

In the limit as the number N of observable random variables approaches infinity, the logarithm of $p(\mathbf{r}_N \mid \mathbf{S}_p)$ is proportional to the metrics $PM(\mathbf{S}_p)$, defined as

$$PM(\mathbf{S}_p) = -\int_{-\infty}^{\infty} \left| r_l(t) - \sum_n S_n h(t - nT) \right|^2 dt$$

$$= -\int_{-\infty}^{\infty} \left| r_l(t) \right|^2 dt + 2\,\mathrm{Re}\left\{ \sum_n \left[S_n^* \int_{-\infty}^{\infty} r_l(t) h^*(t - nT) dt \right] \right\} \tag{46}$$

$$- \sum_n \sum_m S_n^* S_m \int_{-\infty}^{\infty} h^*(t - nT) h(t - mT) dt$$

The maximum-likelihood estimates of the symbols $S_1, S_2 \cdots S_p$ are those that maximize this quantity. Note however that the integral of $\left| r_l(t) \right|^2$ is common to all metrics, and hence, it may be discarded. The third term in Equation (46) is used in the computation of the metrics $PM(\mathbf{S}_p)$, however it does not depend on the received signal $r_l(t)$. Hence, the only integral involving $r_l(t)$ gives rise to the variables

$$y_n \equiv y(nT) \equiv \int_{-\infty}^{\infty} r_l(t) h^*(t - nT) dt . \tag{47}$$

These variables can be generated by passing $r_l(t)$ through a filter matched to $h(t)$ and sampling the output at the symbol rate 1/T. The samples $\{y_n\}$ form a set of

sufficient statistics for the computation of $PM(\mathbf{S}_p)$, hence for the maximum likelihood estimation of the input sequence. Thus, we may conclude that the demodulator implemented as a matched filter to $h(t)$ is information lossless.

By use of the matched filter we may confine our attention to the following discrete-time model

$$y_k = \sum_n S_n x_{k-n} + v_k \tag{48}$$

which results from substituting the expression in (40) for $r_l(t)$ in Equation (47). $x(t)$ is by definition, the response of the matched filter to the input $h(t)$ and

$$x_n = x(nT) = \int_{-\infty}^{\infty} h^*(t)h(t+nT)dt . \tag{49}$$

Hence $x(t)$ represents the output of a filter having an impulse response $h^*(-t)$ and an excitation $h(t)$. In other words, $x(t)$ represents the autocorrelation function of $h(t)$ and $\{x_n\}$ represents the samples of the autocorrelation function, taken periodically at 1/T. v_k denotes the additive noise sequence at the output of the matched filter, thus

$$v_k = \int_{-\infty}^{\infty} z(t)h^*(t-kT)dt . \tag{50}$$

Equation (48) indicates that the output of the demodulator (matched filter) at the sampling instants is corrupted by ISI unless $x_{k-n} = 0$ for $k \neq n$, which is in general not satisfied by $h(t)$ expressed in Equation (41) for our transmit delay based simulcast system. In any practical system, it is reasonable to assume that ISI affects a finite number of symbols. Hence, we may assume that $x_n = 0$ for $|n| > L$ and express the discrete time model as

44

$$y_k = \sum_{n=-L}^{L} x_n S_{k-n} + v_k.$$ (51)

The major difficulty with this discrete time model occurs in the evaluation of performance of various equalization techniques. It is difficult to estimate the performance of the equalizers operating on this model analytically and resort is made to simulation. The difficulty is caused by the correlations in the noise sequence $\{v_k\}$. That is the set of noise variables $\{v_k\}$ in Equation (51) is a Gaussian-distributed sequence with zero-mean and autocorrelation function

$$\frac{1}{2} E\{v_k^* v_j\} = \begin{cases} N_0 x_{j-k} & (|k-j| \le L) \\ 0 & (otherwise) \end{cases}.$$ (52)

The noise sequence is correlated unless $x_k = 0$, $k \ne 0$. Since it is more convenient to deal with the white noise sequence when calculating the error rate performance, it is desirable to whiten the noise sequence by further filtering the sequence $\{y_k\}$. A discrete-time noise-whitening filter is determined as follows.

Let $X(z)$ denote the (two-sided) z transform of the sampled autocorrelation function $\{x_k\}$, i.e.

$$X(z) = \sum_{k=-L}^{L} x_k z^{-k}.$$ (53)

Since $x_k = x_{-k}^*$, it follows that $X(z) = X^*(1/z)$ and the $2L$ roots of $X(z)$ have the symmetry that if ρ is a root, $1/\rho^*$ is also a root. Hence, $X(z)$ can be factored and expressed as

$$X(z) = F(z)F^*(1/z)$$ (54)

where $F(z)$ is a polynomial of degree L having the roots $\rho_1, \rho_2, \ldots \rho_L$ and $F^*(1/z)$ is a polynomial of degree L having the roots $1/\rho_1^*, 1/\rho_2^*, \ldots 1/\rho_L^*$. Assuming that there are no roots on the unit circle, an appropriate noise-whitening filter has a z

45

transform $1/F^*(1/z)$. Since there are 2^L possible choices for the roots of $F^*(1/z)$, each choice resulting in a filter characteristic that is identical in magnitude but different in phase from the other choices, one may choose the unique $1/F^*(1/z)$ that results in an anticausal but stable impulse response with poles corresponding to the zeros of $X(z)$ that are outside of the unit circle. Selecting the noise-whitening filter in this manner ensures that the resulting channel impulse response, characterized by $F(z)$ is minimum phase. Thus the resulting system is both stable and causal and also has a stable and causal inverse since both the poles and zeros of $F(z)$ are inside the unit circle. Consequently, passage of the sequence $\{y_k\}$ through the digital filter $1/F^*(1/z)$ results in an output sequence $\{u_k\}$ that can be expressed as

$$u_k = \sum_{n=0}^{L} f_n S_{k-n} + \eta_k \tag{55}$$

where $\{\eta_k\}$ is a white Gaussian noise sequence having zero-mean and variance N_0 and $\{f_k\}$ is a set of tap coefficients of an equivalent discrete-time transversal filter having a transfer function $F(z)$.

Note that both the whitening filter $1/F^*(1/z)$ and its inverse $F^*(1/z)$ are realizable, and the sufficient statistics $\{y_k\}$ can be recovered by passing $\{u_k\}$ through the inverse filter $F^*(1/z)$. Hence $\{u_k\}$ is also a set of sufficient statistics for estimation of the input sequence.

The cascade of the matched filter, the sampler and the noise-whitening filter is called the whitened matched filter (WMF) and the resulting model in Equation (55) is referred to as the equivalent discrete-time white noise filter model. Figure-14 illustrates the block diagram of the optimum receiver comprising a maximum likelihood sequence estimator at the output of the whitened matched filter. Although we basically followed [21] in the above derivations, the whitened matched filter approach is due to Forney [24].
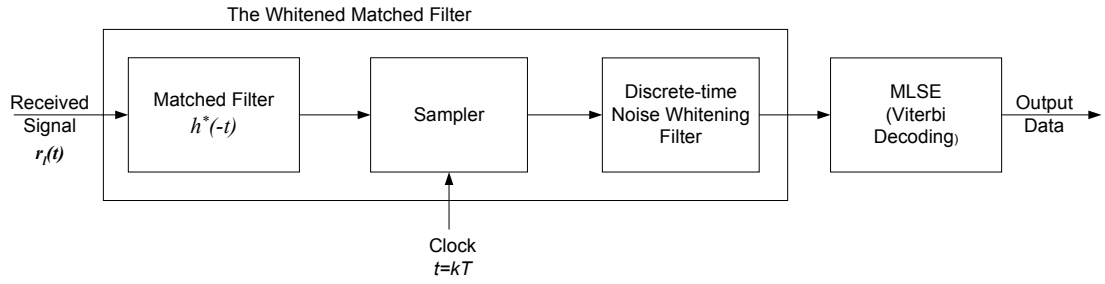
Figure-14 Receiver comprising WMF and MLSE

The output signal to noise ratio is defined to be [24]

$$SNR \equiv \frac{E\left\{\left\|\sum_{n=0}^{L} f_n S_{k-n}\right\|^2\right\}}{N_0} \tag{56}$$

$$= \frac{\|f\|^2}{N_0}$$

where we assumed constant envelope modulation thus $|S_n|^2 = 1$, for all n and

$$\varepsilon_{WMF} \equiv \|f\|^2 \equiv \sum_{n=0}^{L} \|f_n\|^2 \tag{57}$$

corresponds to the received energy for single symbol transmission at the output of the WMF. We refer to this energy ε_{WMF}.

Let us compare the received energy for single symbol transmission obtained from the theoretical evaluations in the previous chapters (denoted by ε) with the symbol energy resulting from the equivalent discrete-time channel based on the whitened matched filter approach (denoted by ε_{WMF}). Recall Figure-10, which depicts the worst case received energy on the transmit delay simulcast network as a function of
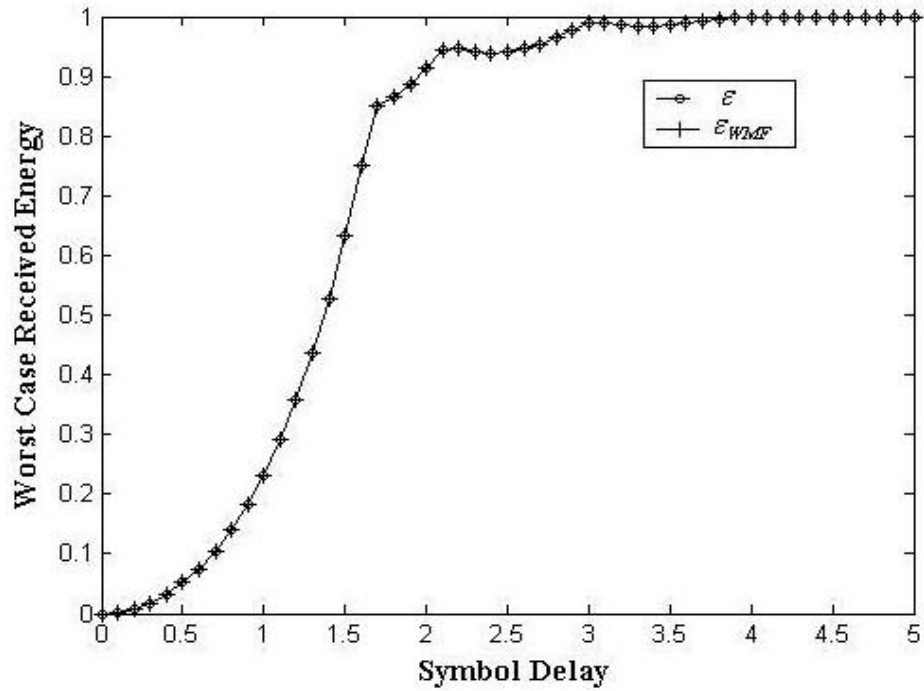
Figure-15 Worst case received energy versus delay introduced between base stations, based on the theoretical evaluations in Chapter 3 and WMF approach, L=3
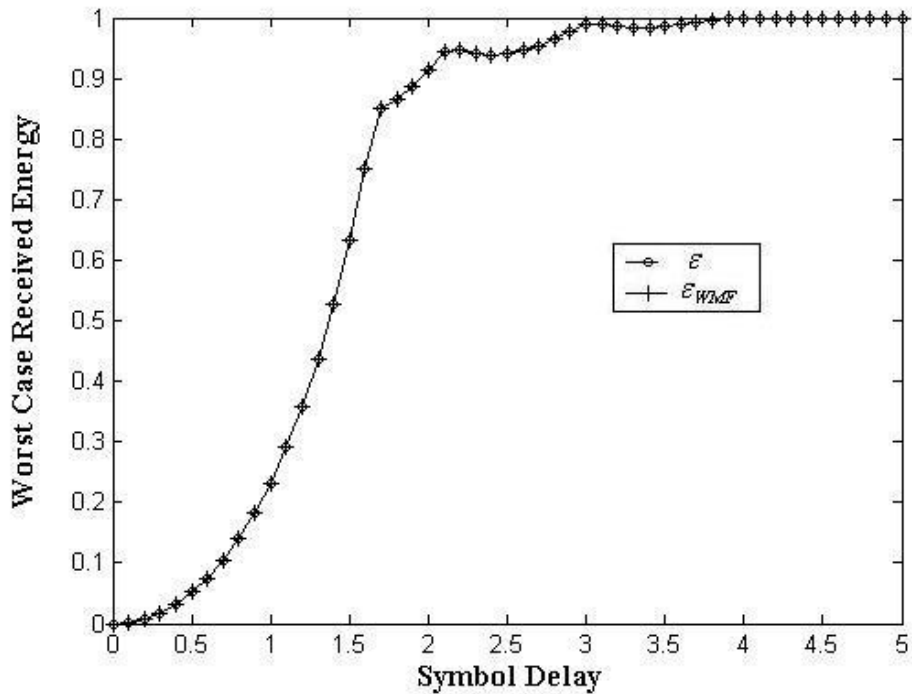
Figure-16 Worst case received energy versus delay introduced between base stations, based on the theoretical evaluations in Chapter 3 and WMF approach, L=5

the delay introduced between base stations assuming LOS propagation. The worst-case received energy was evaluated using the theoretical bound given in Equation (23). The plot for base station separation of 50 km in Figure-10 is redrawn in Figures 15 and 16 for comparison and is signified by ε in the figures. ε_{WMF} is obtained by generating 20000 random mobile positions on the 50 km long axis connecting the two base stations for every transmit delay value. Assuming LOS propagation from both base stations, the equivalent discrete-time white noise filter model is derived for each mobile position, ε_{WMF} is calculated and the least ε_{WMF} is noted as the worst case received energy for this delay value. Figure-15 depicts $\varepsilon_{WMF}$ when L=3, thus the discrete-time model is truncated to four taps and Figure-16 depicts the case when L=5 and the discrete-time model is truncated to six taps. We observe that there is no degradation in received symbol energy when the signal passes through the WMF, which is not surprising in the sense that this is what we would already expect from an optimum demodulator. We also observe that the degradation in received symbol energy that one may expect because of truncating the equivalent channel response to four taps is also not evident in the figures. This is because of the fact that the whitening filter was chosen such that the resulting equivalent discrete-time white noise filter is minimum phase and the minimum phase condition implies that the energy in the first M values of the impulse response $\{f_0, f_1, \ldots, f_M, \ldots, f_L\}$ is a maximum for every M.

4.2 Sub-Optimum Demodulation

The whitened-matched filter approach, although optimum from a probability of error viewpoint, may be disadvantageous in some cases because of the requirement of an adaptive matched filter at the receiver. One may prefer to use a fixed matched filter at the receiver matched to the modulating pulse $g(t)$ and sample the output at the symbol rate 1/T, which would have been the optimum demodulator if the overall channel to the receiver were the additive white Gaussian noise channel without ISI. In this case the received signal given in (40) will pass through the matched filter with impulse response $g^*(-t)$ and sampled at rate 1/T, giving rise to the variables

$$y_n \equiv y(nT) \equiv \int_{-\infty}^{\infty} r_l(t) g^*(t - nT - \Delta) dt \qquad (59)$$

where Δ is the sampling delay. If we substitute for $r_l(t)$ in Equation (59), using Equation (40), we obtain

$$y_k = \sum_n S_n x_{k-n} + v_k \qquad (60)$$

where $x(t)$ is now the response of the matched filter with impulse response $g^*(-t)$ to the input $h(t)$, thus

$$x_n = x(nT) = \int_{-\infty}^{\infty} g^*(t) h(t + nT + \Delta) dt . \qquad (61)$$

and substituting the expression given in (41) for $h(t)$ we result in

$$x(t) = \alpha q(t) + \beta q\big(t - (\tau + \tau_p)\big) \qquad (62)$$

and

$$x_n = x(nT) = \alpha q\big(nT + \Delta\big) + \beta q\big(nT + \Delta - (\tau + \tau_p)\big) \qquad (63)$$

where $q(t)$ is the autocorrelation function of $g(t)$, defined as

$$q(t) = \int g^*(\eta) g(\eta + t) d\eta . \qquad (64)$$

We may again assume that the ISI consists of a finite number of symbols, say L symbols, and rewrite the equivalent discrete time model as

$$y_k = \sum_{n=0}^{L} x_n S_{k-n} + v_k . \qquad (65)$$

Here we assumed that sufficiently large delay is introduced to ensure the causality of the resultant discrete-time system. Thus, in this case the tap-gain coefficients $\{x_0, x_1, \ldots, x_L\}$ of the equivalent discrete-time channel model are determined by

50

sampling $x(t)$ in Equation (62) at L+1 successive instants separated by T. It is reasonable to choose Δ such that the energy in the equivalent discrete-time channel impulse response, given by

$$\varepsilon_{SUB} \equiv \|x\|^2 \equiv \sum_{n=0}^{L} \|x_n\|^2 \tag{66}$$

is maximized. (This corresponds to a certain symbol synchronization criterion.) Here we denote the energy for single symbol transmission with ε_{SUB} to indicate that this is the single symbol energy at the output of the sub-optimum demodulator. v_k in (60) denotes the additive noise sequence at the output of the matched filter, thus

$$v_k = \int_{-\infty}^{\infty} z(t) g^*(t - kT - \Delta) dt .$$

The set of noise variables $\{v_k\}$ is a Gaussian distributed sequence with zero mean and autocorrelation function

$$\frac{1}{2} E\{v_k^* v_j\} = N_0 q_{j-k} = N_0 q((j-k)T)$$

We may let $q(t)$ be a Nyquist pulse, hence $q_{j-k} = 0$ for $j \neq k$. Thus, the set of noise variables $\{v_k\}$ is uncorrelated. The block diagram of a receiver comprising the suboptimum demodulator and MLSE is shown in Figure-17.
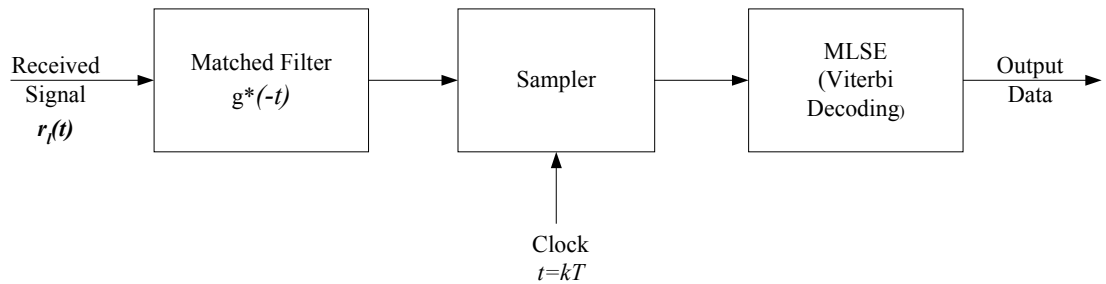
Figure-17 Receiver comprising suboptimum demodulation and MLSE

Let us compare the received energy for single symbol transmission obtained from the theoretical evaluations in the previous chapters with the symbol energy resulting from the equivalent discrete-time channel based on suboptimum demodulation (ε_{SUB}). Figures 18 and 19 are duals of Figures 15 and 16 and depict the worst-case received energies at the output of the suboptimum demodulator, when the channel impulse response is truncated to four and six taps respectively. We observe a general degradation in received energy when compared to the theoretical bound. The degradation is more evident when the symbol delay is integer and half fold of symbol period. This is because of the fact that when the delay between the two paths is a non-integer symbol period value, there is no way for the sampler at rate 1/T to sample both of the signals close to their peak values. The degradation in worst-case received energy due to this phenomenon is not greater than 0.5 dB in Figure-19, which means a relatively small loss in SNR. Moreover we observe a sharp degradation in Figure-18 when the delay introduced between base stations is greater than three symbol periods. This is because with such large transmit delays between the base stations, the propagation delay further increasing the relative delay between the two paths in certain regions, one of the diversity paths falls outside of the four symbol period wide channel window and the equivalent channel model cannot exploit the diversity that inherently resides in this path. This problem may be solved by avoiding unnecessarily large transmit delays between the base stations. Increasing the channel length (as seen from Figure-19) may be another solution, however keeping in mind that increasing the channel length will result in increasing computational complexity at the MLSE.
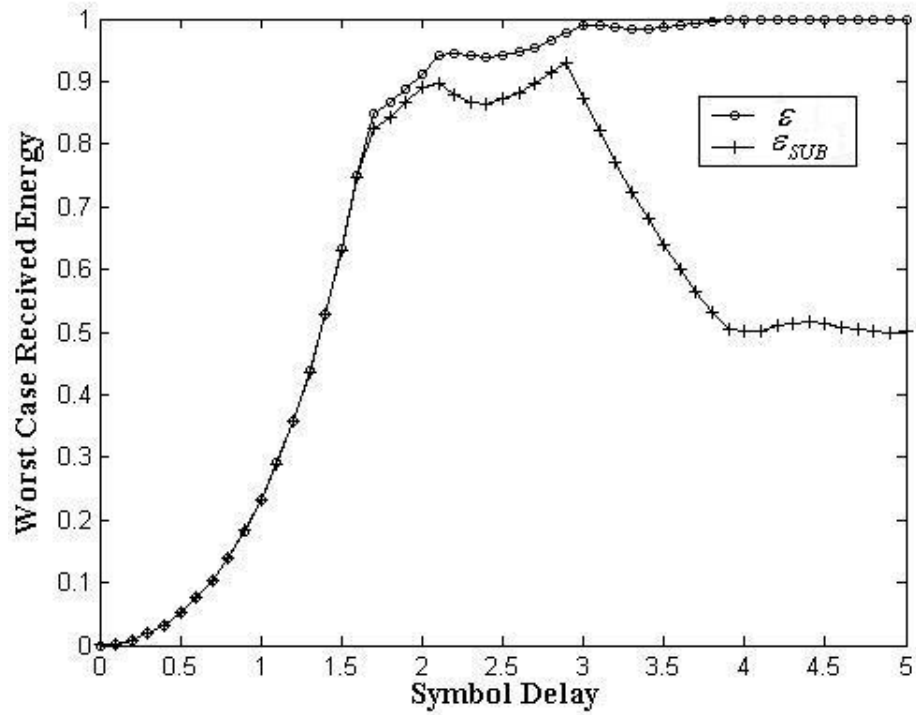
Figure-18 Worst case received energy versus delay introduced between base stations, based on the theoretical evaluations and sub-optimum demodulation, L=3
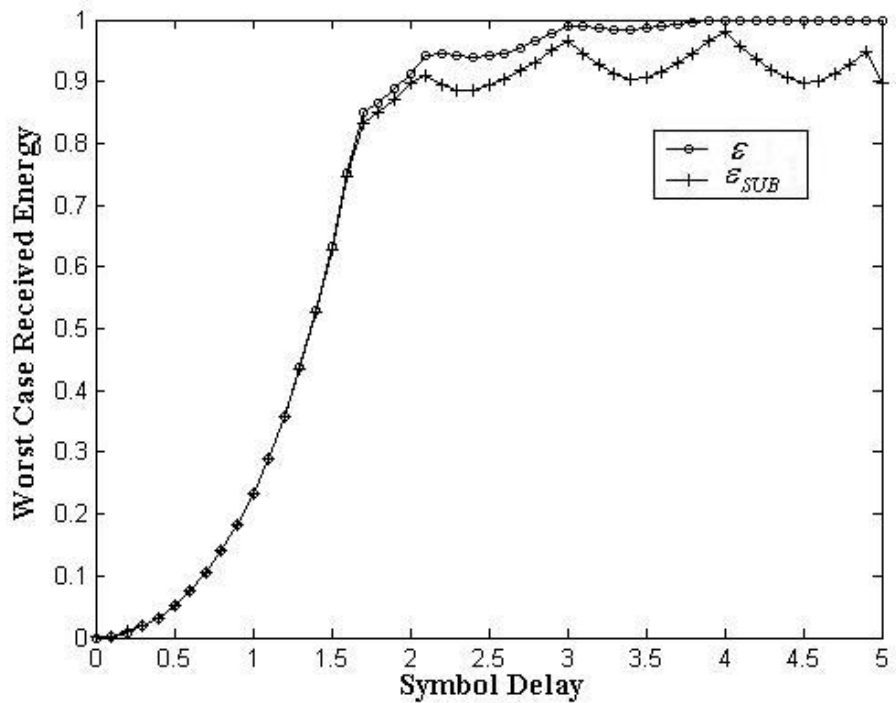
Figure-19 Worst case received energy versus delay introduced between base stations, based on the theoretical evaluations and sub-optimum demodulation, L=5

53

CHAPTER 5

PERFORMANCE OF MLSE

In this chapter, we will derive the performance of MLSE for channels with ISI when the information is transmitted via π/4 DQPSK and describe the algorithm employed to find the *minimum distance* that arises as the fundamental performance parameter for maximum likelihood sequence estimation.

5.1   The Viterbi Algorithm

In the previous chapter, we derived an equivalent discrete-time channel model for the cascade of the analog filter in the transmitter, the channel, the (whitened) matched filter at the receiver and the sampler and expressed our discrete-time model in the general form

$$u_k = \sum_{n=0}^{L} f_n S_{k-n} + \eta_k \tag{66}$$

where $\{f_n\}$ is the set of tap coefficients and $\{\eta_k\}$ is the additive white Gaussian noise sequence with variance N_0.

MLSE of the information sequence $\{S_k\}$ is defined as the choice of that $\{S_k\}$ for which the probability density function $p(\{u_k\}|\{S_k\})$ is maximized. In the presence of ISI that spans $L+1$ symbols (*L* interfering components) the MLSE criterion is equivalent to the problem of estimating the state of a discrete-time finite state machine. The finite-state machine in this case is the equivalent discrete-time channel

with coefficients $\{f_n\}$, and its state at any time instant is given by the L most recent inputs. Hence if the information symbols are *M*-ary, the channel filter has M^L states. Consequently, the channel is described by an M^L state trellis and the Viterbi algorithm may be used to determine the most probable path through the trellis [21].

Here we will not go into the details of the well-known Viterbi algorithm, but only note that the algorithm provides an efficient means for recursively estimating the information sequence $\{S_k\}$ from the output sequence $\{u_k\}$. When the additive noise terms $\{\eta_k\}$ are independent and Gaussian distributed, the metrics computed recursively in the Viterbi algorithm can be expressed as

$$PM_{k-L}(\mathbf{S}_k) = PM_{k-L-1}(\mathbf{S}_{k-1}) - \left| u_k - \sum_{n=0}^{L} f_n S_{k-n} \right|^2 \tag{67}$$

and the maximum likelihood estimates of $\{S_k\}$ are those that maximize this metrics. This metrics expression will constitute a starting point for the performance analysis in the following section.

In the beginning of this thesis work a maximum likelihood sequence estimator using the Viterbi algorithm was implemented for $\pi/4$ DQPSK modulation and we tried to determine the bit error rate of the transmit delay scheme by Monte Carlo simulations. Determining the bit error rate with Monte Carlo simulations requires large computation times, especially at low bit error rates. The problem gets even more severe when one would like to investigate the coverage properties of a network and the channel at a given position on the network is itself random, which is the case with Rayleigh fading. Hence, the problem of large computation times directed us to determine the performance of MLSE analytically for $\pi/4$ DQPSK and use the results of the theoretical derivations.

5.2 Performance of MLSE for Channels with ISI

In this section, we shall determine the probability of error for MLSE of the received information sequence when the information is transmitted via π/4 DQPSK. We will basically follow the derivation in [21], where real PAM signaling is considered. The derivation in [21] applies for π/4 DQPSK with some modification.

In π/4 DQPSK, the complex modulation symbol S_k may take one of the four values

$$S_{odd} = \left\{ \frac{1}{\sqrt{2}} + j\frac{1}{\sqrt{2}}, \quad -\frac{1}{\sqrt{2}} + j\frac{1}{\sqrt{2}}, \quad -\frac{1}{\sqrt{2}} - j\frac{1}{\sqrt{2}}, \quad \frac{1}{\sqrt{2}} - j\frac{1}{\sqrt{2}} \right\} \tag{68}$$

for odd symbol numbers and one of the four values

$$S_{even} = \left\{ 1, \quad j, \quad -1, \quad -j \right\} \tag{69}$$

for even symbol numbers. The trellis has 4^L states, defined at time k with the L most recent symbol inputs, thus

$$Z_k = (S_{k-1}, S_{k-2}, \ldots S_{k-L}) \tag{70}$$

where S_k takes values from either the odd symbol number set or even symbol number set depending on the symbol number k. Let the estimated symbols from the Viterbi algorithm be denoted by $\{\widetilde{S}_k\}$ and the corresponding estimated state at time k by

$$\widetilde{Z}_k = (\widetilde{S}_{k-1}, \widetilde{S}_{k-2}, \ldots \widetilde{S}_{k-L}). \tag{71}$$

If we suppose that the estimated path through the trellis diverges from the correct path at time k and remerges with correct path at time $k+l$, this will mean that $\widetilde{S}_k \neq S_k$ and $\widetilde{S}_{k+l-L-1} \neq S_{k+l-L-1}$. This is called an error event and can be represented by a corresponding doubly infinite error sequence e as,

$$e = (\ldots 0, 0, e_k, e_{k+1}, \ldots e_{k+l-L-1}, 0, 0 \ldots) \tag{72}$$

56

where the error sequence is characterized by the properties that $e_j = 0$ for $j < k$ and $j > k+l-L-1$, $e_k \neq 0$, $e_{k+l-L-1} \neq 0$ and there is no sequence of L consecutive elements in the interval $k \leq m \leq k+l-L-1$ that are zero. These properties come from our starting assumption for the error event. The components of ε are defined as

$$e_j = \left(S_j - \widetilde{S}_j \right). \tag{73}$$

With π/4 DQPSK, the corresponding sets of all possible symbol differences are

$$e_{odd} = \left\{ \begin{array}{l} -\sqrt{2}, \quad -j\sqrt{2}, \quad -\sqrt{2}-j\sqrt{2}, \quad -\sqrt{2}+j\sqrt{2}, \quad 0, \\ \sqrt{2}-j\sqrt{2}, \quad \sqrt{2}+j\sqrt{2}, \quad j\sqrt{2}, \quad \sqrt{2} \end{array} \right\} \tag{74}$$

for odd symbol numbers and

$$e_{even} = \left\{ -2, \quad -j2, \quad -1-j, \quad -1+j, \quad 0, \quad 1-j, \quad 1+j, \quad j2, \quad 2 \right\} \tag{75}$$

for even symbol numbers and e_j may take values from one of these sets depending on whether j is even or odd.

We would like to determine the probability of occurrence of the error event that begins at time k and is characterized by the error sequence e given in Equation (72). Specifically for the error event e to occur, the following three subevents E_1, E_2, E_3 must occur:

E_1 : At time k, $\widetilde{Z}_k = Z_k$.

E_2 : Remembering the definition in (73), the error sequence $e = (...0, e_k, e_{k+1}, ..., e_{k+l-L-1}, 0...)$ when subtracted from the modulation symbol sequence $S = (...S_k, S_{k+1}, ...S_{k+l-L-1}...)$ must result in an allowable sequence, i.e., the resulting sequence $\widetilde{S} = (...\widetilde{S}_k, \widetilde{S}_{k+1}, ...\widetilde{S}_{k+l-L-1}...)$ must be allowable in the sense that its elements $\widetilde{S}_i$ must have values selected from S_{odd} and S_{even} sets, depending on the symbol number k.

E_3 : For $k \le m < k + l$, the sum of the branch metrics of the estimated path exceeds the sum of the branch metrics of the correct path.

The probability of occurrence of E_3 is

$$P(E_3) = P\left[\sum_{i=k}^{k+l-1}\left|u_i - \sum_{j=0}^{L} f_j \widetilde{S}_{i-j}\right|^2 < \sum_{i=k}^{k+l-1}\left|u_i - \sum_{j=0}^{L} f_j S_{i-j}\right|^2\right] \tag{76}$$

However,

$$u_i = \sum_{n=0}^{L} f_n S_{i-n} + \eta_i \tag{77}$$

where $\{\eta_i\}$ is a complex valued white Gaussian noise sequence. Substitution of Equation (77) in Equation (76) yields

$$P(E_3) = P\left[\sum_{i=k}^{k+l-1}\left|\eta_i + \sum_{j=0}^{L} f_j e_{i-j}\right|^2 < \sum_{i=k}^{k+l-1}|\eta_i|^2\right]$$

$$= P\left[\sum_{i=k}^{k+l-1} 2\,\mathrm{Re}\left\{\eta_i^*\left(\sum_{j=0}^{L} f_j e_{i-j}\right)\right\} < -\sum_{i=k}^{k+l-1}\left|\sum_{j=0}^{L} f_j e_{i-j}\right|^2\right] \tag{78}$$

Let us define

$$\alpha_i = \sum_{j=0}^{L} f_j e_{i-j} \tag{79}$$

then Equation (78) may be expressed as

$$P(E_3) = P\left[\sum_{i=k}^{k+l-1} 2\,\mathrm{Re}\left\{\eta_i^* \alpha_i\right\} + \sum_{i=k}^{k+l-1}|\alpha_i|^2 < 0\right] \tag{80}$$

$$= P(U < 0)$$

where U refers to the left side of the inequality in the probability parenthesis in (80). U is a linear combination of statistically independent Gaussian random variables, hence is Gaussian distributed with mean

58

$$E\{U\} = \sum_{i=k}^{k+l-1} |\alpha_i|^2 \qquad (81)$$

and variance

$$\text{Var}\{U\} = 4N_0 \sum_{i=k}^{k+l-1} |\alpha_i|^2 . \qquad (82)$$

For these values of mean and variance, the probability that U is less than zero is simply

$$P(E_3) = Q(\sqrt{\frac{\sum_{i=k}^{k+l-1} |\alpha_i|^2}{4N_0}}) \qquad (83)$$

It is convenient to define,

$$d^2(e) \equiv \sum_{i=k}^{k+l-1} |\alpha_i|^2 = \sum_{i=k}^{k+l-1} \left| \sum_{j=0}^{L} f_j e_{i-j} \right|^2 = \|f * e\|^2 \qquad (84)$$

and express (83) as

$$P(E_3) = Q(\sqrt{\frac{d^2(e)}{4N_0}}) . \qquad (85)$$

Note that $d^2(e)$ may be expressed as the squared l_2 norm of the sequence resulting from the convolution of the channel tap-coefficient sequence $\{f_n\}$ with the error sequence e. Expressing $d^2(e)$ in this form will be useful in the following section.

The subevent E_2 is independent from subevents E_1 and E_3, and depends only on the statistical properties of the input sequence. We assume that the information symbols are equally probable and that the symbols in the transmitted sequence are statistically independent. Let S_e denote the set of all possible input sequences S that satisfy the rule for subevent E_2, thus when the error sequence e is subtracted from the input

59

sequence $S \in S_e$, the result is an allowable sequence $\widetilde{S}$. Then, the probability for subevent E_2 may be expressed as

$$P(E_2) = \sum_{S \in Se} P(S) \tag{86}$$

Note that the number of allowable symbols S_i corresponding to the error e_i depend on the value of e_i. Let us consider the error set e_{even} for even symbol numbers given by Equation (75). e_i may take the value 0 for every element S_i of the even symbol set S_{even} given in Equation (69), while for each of the error values $-1-j$, $-1+j$, $1-j$ and $1+j$ there are only two possible values for S_i such that

$$S_i = \widetilde{S}_i + e_i,$$

moreover, when the error value e_i takes one of the values -2, $-2j$, $2j$ or 2, corresponding to each of these values there is only a single possible value for S_i. Thus, there is no closed form formula for $P(E_2)$ with $\pi/4$ DQPSK. All the allowable input symbol sequences S and their corresponding probabilities should be carefully calculated for the given error sequence e.

The probability of subevent E_1 is much more difficult to compute exactly because of its dependence on subevent E_3, however it is well approximated (and upper-bounded) by unity for low symbol error probabilities. Therefore, the probability of the error event e is well approximated and upper-bounded as

$$P(e) \leq Q(\sqrt{\frac{d^2(e)}{4N_0}}) \sum_{S \in Se} P(S). \tag{87}$$

Having determined an upper bound for the probability of occurrence of the given error event e, we will now try to find out an expression for the bit error probability of MLSE of $\pi/4$ DQPSK. Let E be the set of all non zero error events e starting at time k and let $w(e \mid S)$ be the corresponding number of bit errors in each error event e given the input symbol sequence is S. Note that with differential encoding the

60

number of bit errors resulting from the error sequence e do not only depend on the error sequence but also on the input symbol sequence. $w(e \mid S)$ must be carefully calculated, considering that the modulation sequence is encoded differentially. The probability of a bit error is upper-bounded (union bound) as

$$P_b \leq \sum_{e \in E} Q(\sqrt{\frac{d^2(e)}{4N_0}}) \sum_{S \in Se} \frac{1}{2} w(e \mid S) P(S) \tag{88}$$

where the factor ½ appears because we consider quaternary signaling and thus, two bits are encoded into a single symbol. The computation of P_b may be simplified by focusing on the dominant term in the summation in Equation (88). Because of the exponential dependence of the each term in the sum, the expression P_b is dominated by the term corresponding to the minimum value of d^2, denoted as $d_{\min}^2$. $d_{\min}^2$ may be formally defined as

$$d_{\min}^2 \equiv \min_{e \in E} \|f * e\|^2 \tag{89}$$

where the minimization is over the set E of all possible nonzero sequences e. Denoting the set of error events for which $d^2(e) = d_{\min}^2$ by $E_{d_{\min}^2}$, the bit error probability may be approximated as

$$P_b \cong K_{d_{\min}^2} Q(\sqrt{\frac{d_{\min}^2}{4N_0}}) \tag{90}$$

where

$$K_{d_{\min}^2} = \sum_{e \in E_{d_{\min}^2}} \sum_{S \in Se} \frac{1}{2} w(e \mid S) P(S). \tag{91}$$

Note that in the absence of ISI, $d_{\min}^2$ will be realized for minimum magnitude single error events. Thus,

$$d_{\min}^2 = \|f\|^2 \|\varepsilon_i\|_{\min}^2 = 2\|f\|^2 = 2\varepsilon,$$

remembering that the energy at the output of the matched filter is equal to the received symbol energy ε when optimum demodulation is considered. Thus, in the absence of ISI, the P_b resulting from Equation (90) is proportional to the bit error probability for π/4-DQPSK given by Equation (20) as

$$P_b = 2Q(\sqrt{\frac{\varepsilon}{2N_0}}) \, .$$

In fact it can be shown that considering all possible minimum magnitude single error events the coefficient $K_{d_{\min}^2}$ given by Equation (91) evaluates to 2 and hence the P_b expression in Equation (90) results exactly in the bit error probability for π/4-DQPSK given in Equation (20) when there is no ISI.

5.3   Finding the Minimum Distance for MLSE

In the previous section, we have seen that the performance of maximum likelihood sequence estimation (MLSE) basically depends on the minimum distance $d_{\min}^2$ defined by Equation (89). In this equation, $d_{\min}^2$ is defined as a minimization over all possible error sequences (signal pair differences). Since there are an infinite number of possible error sequences, to determine the error sequence with $d_{\min}^2$ we must use a search technique that limits the number of error sequences to be examined. The search technique used in this thesis is based on the tree-pruning algorithm suggested in [26].

The technique suggested in [26] stems from a combined functional analysis-computer search approach. Several theoretical observations, which point out symmetries of various kinds, bring a distillation within the scope of the computer that selects the crucial error patterns from the full tree of error patterns, based on these observations. The theoretical results are derived in Reference [25] where the authors develop a universal procedure for finding $d_{\min}^2$ when M-ary PAM data is transmitted over all

real channels of memory L. Reference [26] adopts this algorithm to find $d^2_{\min}$ for a given specific channel of memory L. Both of the papers consider M-ary signaling over real channels. Since we consider $\pi/4$-DQPSK, in this thesis the algorithm in [26] is generalized for complex signaling over complex channels.

Let us restate our problem: We would like to determine the minimum distance, $d^2_{\min}$ for a given finite memory channel $f = \cdots 0, f_0, f_1, \cdots, f_L, 0 \cdots$, where f_i are complex in general and $f_0 f_L \neq 0$ so that we can say the channel memory is L. The definition of $d^2_{\min}$ is

$$d^2_{\min} \equiv \min_{e \in E} \|f * e\|^2$$

where the minimum is over the set E of all nonzero sequences e of the form $\cdots 00 e_0 e_1 \cdots e_K 00 \cdots$, where K is an arbitrary nonnegative integer and e_k is an element of one of the symbol pair difference sets given in (74) and (75) depending on k.

Now we will represent the error sequence e in some alternative forms that will prove to be useful in developing the algorithm. The error sequence $\overbrace{0 \cdots 0}^{L} e_0 \cdots e_K \overbrace{00 \cdots 0}^{L}$ can be expressed as $\Delta_1, \Delta_2, \Delta_3, \cdots, \Delta_{K+L+1}$, where the states Δ_j are defined as the successive L-tuples of the sequence representation, where the first all zero L-tuple is omitted. That is,

$$\overbrace{(0 \cdots 0, 0, e_0)}^{\Delta_1}, \overbrace{(0 \cdots 0, e_0, e_1)}^{\Delta_2}, \cdots, \overbrace{(e_K, 0, 0 \cdots 0)}^{\Delta_{K+L}}, \overbrace{(0, 0, 0 \cdots 0)}^{\Delta_{K+L+1}}.$$

Alternatively the error sequence can be represented by the so-called augmented state representation $\Delta^+_1, \Delta^+_2, \Delta^+_3, \cdots, \Delta^+_{K+L+1}$, where the augmented states Δ^+_j are defined as the successive $(L+1)$-tuples of the sequence representation

63

$$\overbrace{(0\cdots0,0,e_0)}^{L+1},\overbrace{(0\cdots0,e_0,e_1)}^{L+1},\cdots,\overbrace{(e_K,0,0\cdots0)}^{L+1}.$$

This later representation derives its usefulness from the equality

$$\sum_{j=1}^{K+L+1}\left\langle f^b,\Delta_j^+\right\rangle^2 =\left\|f*e\right\|^2 = d(e) \tag{92}$$

where $f^b\equiv(f_L,f_{L-1},\cdots,f_0)$ and the inner product is defined in the usual way.

It can be easily show that

$$\left\|f*e\right\|^2 =\left\|f*(-e)\right\|^2 =\left\|f*(je)\right\|^2 =\left\|f*(e^{*b})\right\|^2 =\left\|f*(-je)\right\|^2 =\left\|f*(-e^{*b})\right\|^2$$
$$=\left\|f*(je^{*b})\right\|^2 =\left\|f*(-je^{*b})\right\|^2$$
$$\tag{93}$$

where the negative, multiplication with j and conjugate backward operations on the sequence $e=(e_0,e_1,\cdots,e_K)$ are defined as follows

$$-(e_0,e_1,\cdots,e_K)\equiv(-e_0,-e_1,\cdots,-e_K)$$
$$j(e_0,e_1,\cdots,e_K)\equiv(je_0,je_1,\cdots,je_K)$$
$$(e_0,e_1,\cdots,e_K)^b\equiv(e_K^*,e_{K-1}^*,\cdots,e_0^*)$$

where * denotes conjugation.

We begin by describing the correspondence between the set of all possible error sequences and a tree with nine branches at each node. The number nine comes because we have nine possible values for the error in both e_{even} and e_{odd} sets. The nodes occur at successive integral heights so that at level one there are nine branches, and in general in height l, there are 9^l branches. We associate a state to each node and an error value to each branch, so that the state of each node is an L-tuple that shows the error values on the L-most recent branches that have been followed to reach the node. Note that since the error sets for even and odd symbol numbers are different for $\pi/4$-DQPSK, the error values associated to the branches at a certain

64

level are chosen from the even error set, if the error values at the previous level were chosen from the odd error set and vice versa. The root node is associated to an all zero state, such as $z = (0,0,\ldots 0)$. The part of the tree that issues upward from a node is called the growth of the node. The growth from each node in the tree, whose state is the all zero state z, is pruned. The nodes that have no growth are termed terminal nodes. Via this labeling we now make the obvious identification that the error values on the branches traversed from the root node to a terminal node correspond to an error sequence and by this way, all the error sequences are represented on the tree.

We define a cost for the transition from a node at height $k-1$ to another node at the successive height k that is connected to the current node with a branch as,

$$c_k \equiv \left\langle f^b, \Delta_k^+ \right\rangle^2 \qquad (94)$$

where the augmented state is the $L+1$-tuple formed by concatenating the state of the departure node and the error value on the transited branch. The cost of a node at height K is defined as

$$C_K = \sum_{i=1}^{K} c_i . \qquad (95)$$

Note that the cost of a terminal node is equal to $d(e)$ for the corresponding error sequence e.

5.3.1 Rules for Pruning the Growth from a Node

We now give some rules with which it is possible to trace the tree by spending an "acceptable" amount of computation effort.

1. Prune the growth of the nodes at level one that are connected to the root node by a branch with a corresponding error value that is the negative, complex conjugate or negative complex conjugate of another branch at the same level.

(That is, if one is to start with the even number set for example, it is enough to trace the growth of only two nodes connected to the root node, say by $1+j$ and 2. The error sequences resulting from the growth of the pruned nodes would simply be the negative, complex conjugate or negative complex conjugate of the error sequences resulting from the growth of the remaining nodes.)

2. If you come to a node with a state Δ_k that is previously encountered on the way from the root to this node, prune the growth from this node. Do the same if the state $\Delta_k = -\Delta_l$ or $\Delta_k = \pm j\Delta_l$ when Δ_l is a previously encountered state.

3. If a node at height l is such that $\Delta_l = \pm\Delta_i^{*b}$, or $\Delta_l = \pm j\Delta_i^{*b}$ for $i \le l$, delete the growth from this node except the continuation that culminates the state representation

$$\Delta_1 \Delta_2 \ldots \Delta_i \Delta_{i+1} \ldots \Delta_{l-1} \left(\pm \Delta_i^{*b}\right) \ldots \left(\pm \Delta_2^{*b}\right)\left(\pm \Delta_1^{*b}\right)$$

or

$$\Delta_1 \Delta_2 \ldots \Delta_i \Delta_{i+1} \ldots \Delta_{l-1} \left(\pm j\Delta_i^{*b}\right) \ldots \left(\pm j\Delta_2^{*b}\right)\left(\pm j\Delta_1^{*b}\right)$$

If $i = l$ then the $\Delta_{i+1}, \ldots \Delta_{l-1}$ segment is vacuous.

And finally,

4. Prune the growth of a node if it costs more than some other previously reached terminal node.

The first three rules may be referred as symmetry rules since they are based on the various symmetry observations given in Equation (93). It may not be apparent that these symmetry rules leave at least one error event at the list that achieves $d_{\min}^2$. That they do follows from the fact that each of these rules prune the growth of a node and discard certain possible error sequences only when there is lower or equal cost error sequence left on the tree. The proofs that they do are quite straightforward and can be found in Reference [25].

CHAPTER 6

PERFORMANCE OF RECEIVERS WITH MLSE

In this chapter, we will investigate the performance of a receiver employing maximum likelihood sequence estimation in a transmit delay based simulcast environment. In Chapter 3, we have evaluated the performance of the scheme based on received symbol energy and have not been interested in specific receiver models that will be employed in the mobile terminals. We have derived these receiver models in Chapters 4 and 5 and now we would like to investigate whether these receiver models reach the theoretically derived performance bounds or not.

In this chapter we will investigate the performance of the scheme with two different receiver models, one employing the optimum demodulator and the other one employing the sub-optimum demodulator, both introduced in Chapter 4. We will employ a maximum likelihood sequence estimator at the outputs of the demodulators and try to find out how the coverage plots given in Chapter 3 are affected by further minimum distance degradations due to MLSE procedure. We will again consider the two different channel models, the LOS channel and the Rayleigh fading channel, both introduced in Chapter 3.

6.1 Definitions

The simulation results will be presented for two different receiver models. The first receiver model employs a WMF as a demodulator and a maximum likelihood sequence estimator at the output of the demodulator (see Figure-14). Remember Chapter 4, where we have emphasized that this is the optimum maximum likelihood receiver for channels with ISI. We will refer to this optimum receiver as Receiver 1.

The second receiver comprises a sub-optimum demodulator and a maximum likelihood sequence estimator and will be referred as Receiver 2 (see Figure-17).

6.2 Performance Evaluation in LOS Propagation Environment

In parallel to Chapter 3, we will use the minimum distance d_{min}^2 itself as a performance measure in LOS propagation environment. The minimum distance is directly related to the bit error probability with the expression given in Equation (90) for MLSE of $\pi/4$ DQPSK modulation. In the figures presented in this section, d_{min}^2 is normalized by dividing it by two since the minimum difference between symbol pairs is $\sqrt{2}$ for DQPSK modulation. Note that the normalized d_{min}^2 is equal to the received symbol energy in the absence of ISI.

Let us investigate whether the worst case received symbol energies depicted at the outputs of the demodulators in Chapter 4, are further degraded by minimum distance reductions in the MLSE procedure. Figure-20 and 21 depict the worst-case minimum distances d_{min}^2 over a two base station simulcast network when Receiver 1 is employed at the mobile. The base station separation is 50 km and as usual we consider only the points on the axis connecting the two base stations. To determine the worst d_{min}^2 on the network, for each transmit delay value we generated 20000 random mobile locations on the radial axis, and we determined the channel for each mobile location and the corresponding discrete-time whitened matched filter model. For each discrete-time channel, we used the algorithm described in the previous chapter to determine the minimum distance over all possible error sequences. Among the 20000 channels corresponding to 20000 different mobile locations the one with minimum d_{min}^2 determined the worst case d_{min}^2 for that transmit delay value. Together with d_{min}^2, the Figures-20 and 21 also depict the variation of the theoretically derived received symbol energy denoted by ε and the symbol energy at the output of the WMF denoted by ε_{WMF} for comparison. An 8-state Viterbi decoder is employed for the results given in Figure-20 and the performance of a 32-state Viterbi decoder is plotted in Figure-21. We observe that there is no degradation in
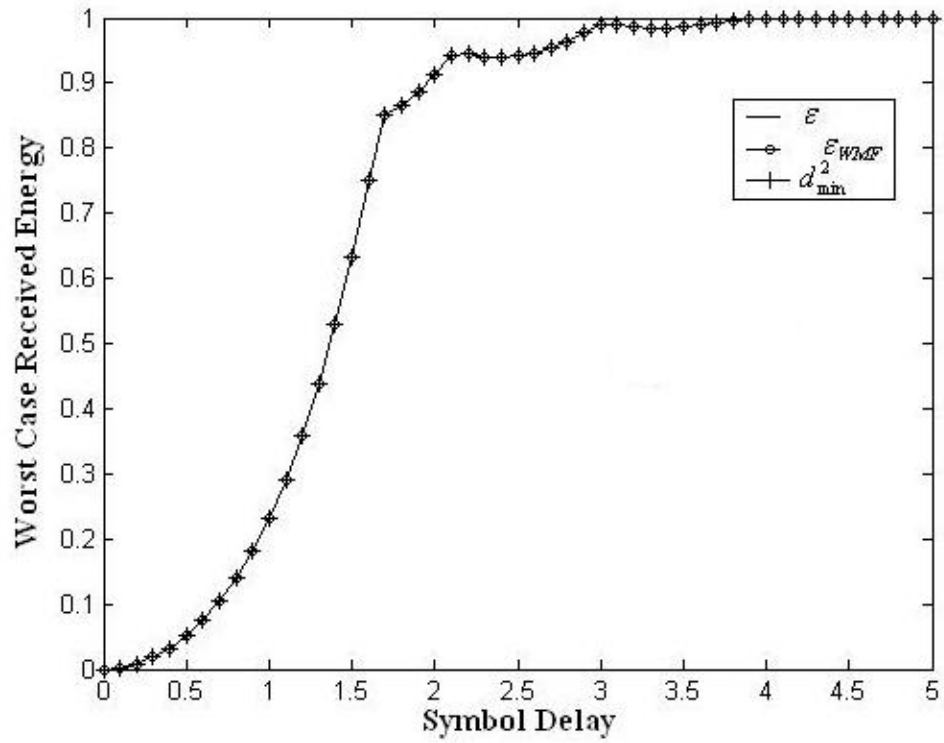
Figure-20 Worst case $d_{\min}^2$ versus delay introduced between base stations with an 8-state Viterbi decoder employed in Receiver 1
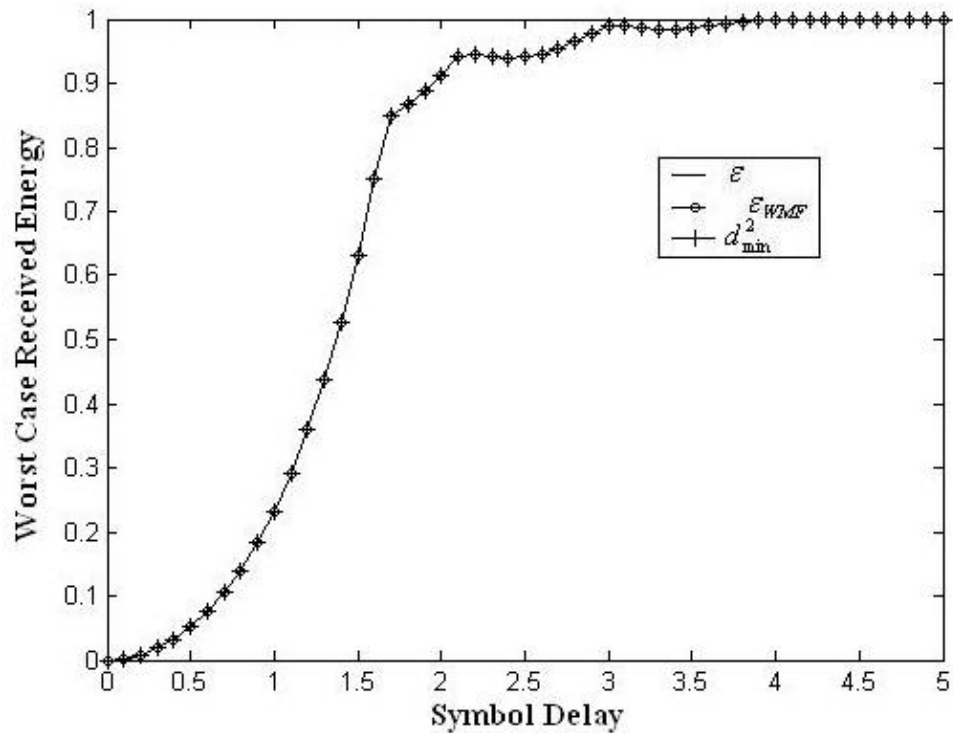
Figure-21 Worst case $d_{\min}^2$ versus delay introduced between base stations with a 32-state Viterbi decoder employed in Receiver 1
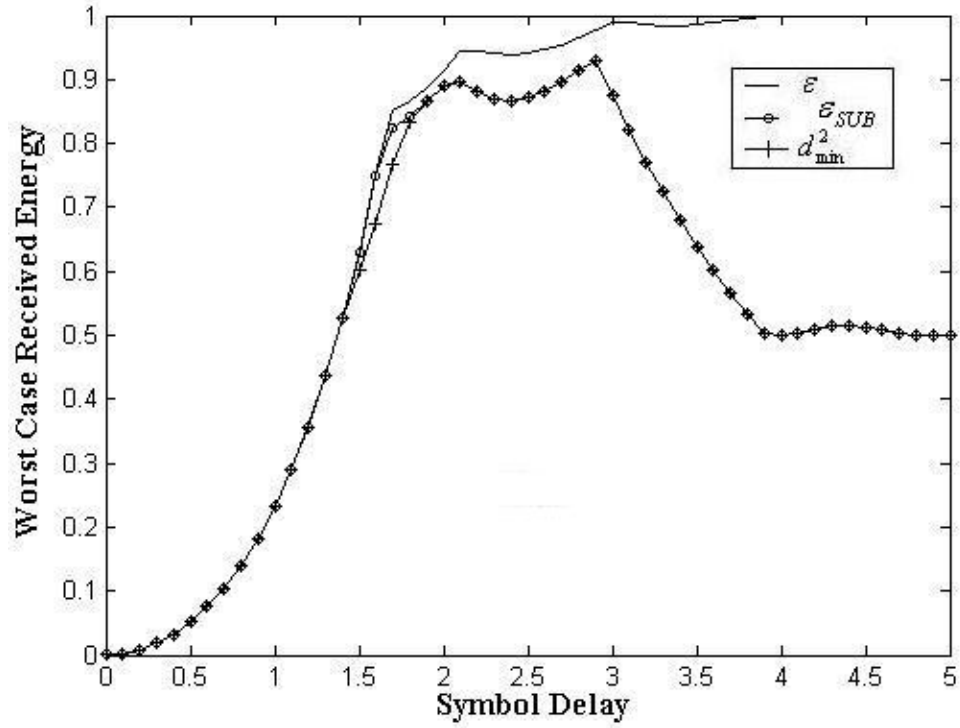
Figure-22 Worst case d_{min}^2 versus delay introduced between base stations with an 8-state Viterbi decoder employed in Receiver 2
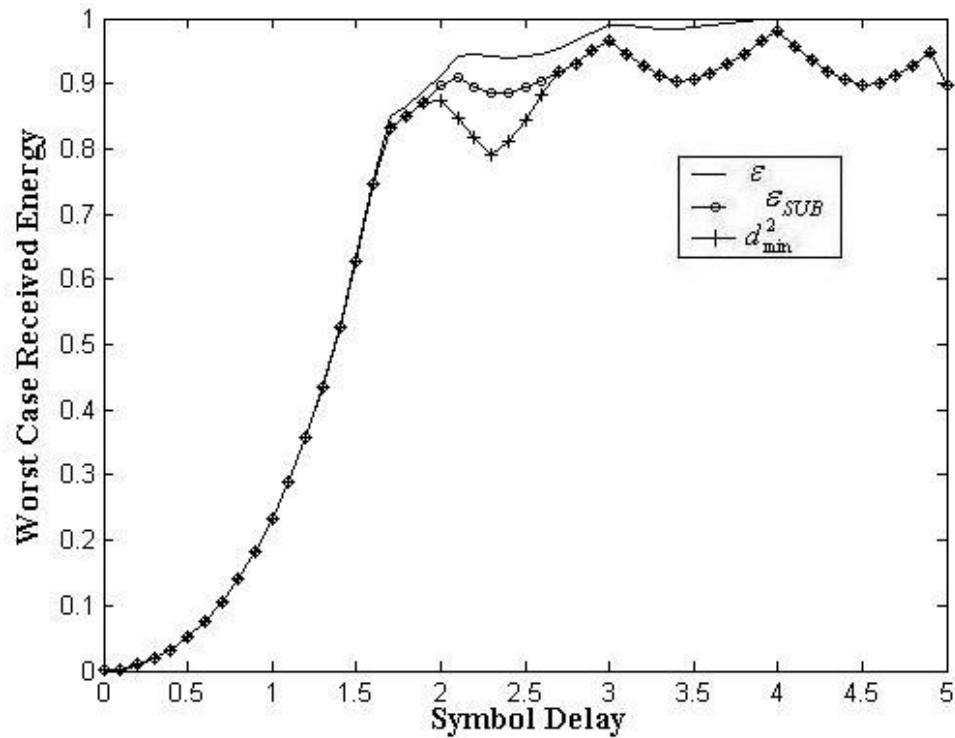

Figure-23 Worst case d_{min}^2 versus delay introduced between base stations with a 32-state Viterbi decoder employed in Receiver 2

70

the worst-case received energies due to MLSE procedure, or more precisely stated due to ISI. However, the plots should not be interpreted as there is absolutely no degradation over the network due to ISI. Instead, one should comment that the degradations due to ISI occur in channels with good performance, that is with high received energies, and so are not evident in worst case plots.

Figures-22 and 23 are duals of Figures-20 and 21 and depict the worst case values for the received symbol energy (theoretical), the single symbol energy at the output of the sub-optimum demodulator and $d_{\min}^2$ as a function of the delay introduced between base stations when Receiver 2 is employed at the mobile. We now observe degradation in the minimum distance for certain delay values. We may again comment that degradations due to MLSE occur at rather 'good' channels for the other delay values and are not evident in the worst case plots. Note that the delay values for which the degradation due to MLSE is evident in worst case received energy plots, depend on the length of the equivalent discrete-time channel or equivalently the number of states in the Viterbi decoder.

6.3 Performance Evaluation in Rayleigh Fading Environment

In this section we will investigate the performance of Receivers 1 and 2 in Rayleigh fading environment. In parallel to Chapter 3, we will use mean bit error probability as a performance measure. In Chapter 3, we have derived the mean bit error probability for two beam Rayleigh fading theoretically and investigated the coverage properties of the scheme based on this derivation. Unfortunately, it is extremely difficult to obtain a closed form expression for the performance of MLSE receiver in Rayleigh fading environment, hence we have performed Monte Carlo simulations. In order to determine the mean bit error probability at a given mobile position, we generate 50 000 random channels for that mobile position according to the Rayleigh distribution and determine the equivalent discrete-time model for each channel. $d_{\min}^2$ is determined for each discrete-time channel by performing a search over all possible error sequences and is used in the bit error probability expression for MLSE given by Equation (90). The resulting bit error probabilities for the ensemble of 50 000

channels are averaged to determine the mean bit error probability for that mobile position. Unfortunately, this procedure requires significant computation times and we would not be able to investigate the coverage properties of the scheme as a function of the delay introduced between base stations. Instead we have investigated the performance of the scheme and the degradation in performance due to MLSE for a fixed transmit delay between base stations. We assume that 1.5 symbol period delay is introduced between the 50 km separated base stations and investigate the variation of the mean bit error probability with mobile location. This case was previously investigated theoretically and results were presented in Figure-11. In Figures-24 and 25 we redraw this plot for comparison and refer to it as 'Theory'. In the figures together with the MLSE and 'Theory' plots, the mean bit error probabilities considering the received symbol energy at the output of the demodulators are also presented. These plots are referred to as 'No ISI' since they reflect the degradation in performance due to discretization but do not include the degradation in performance due to minimum distance reductions in the MLSE procedure. Considering Figures-24 and 25 we observe that the results for the MLSE receiver meet the theoretical expectations quite well.
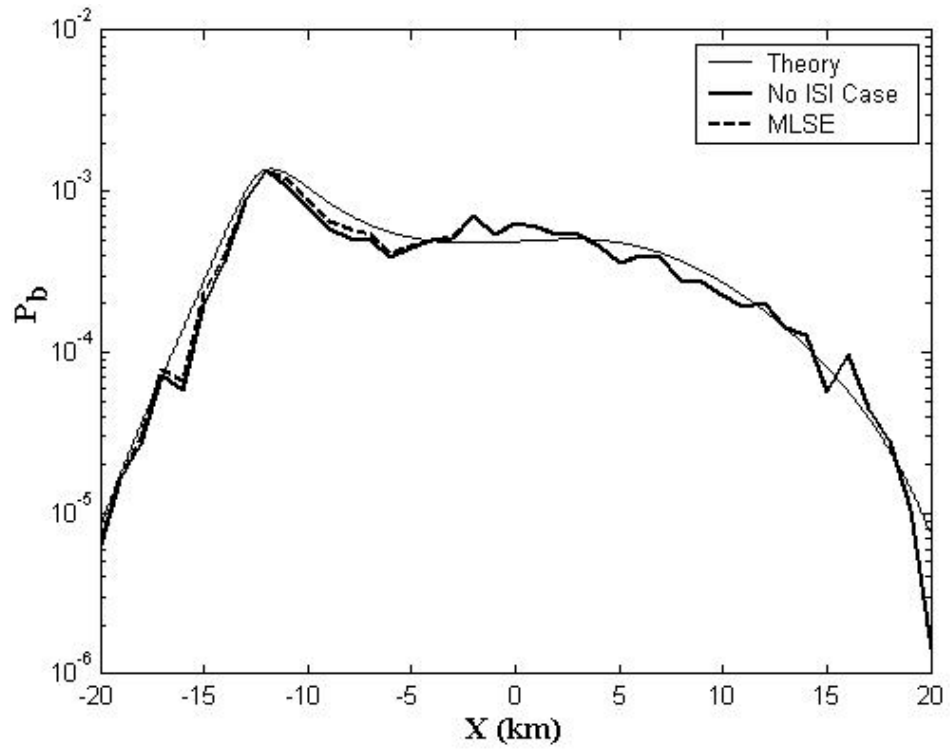
Figure-24 P_b versus mobile position with a 32-state Viterbi decoder employed in Receiver 1
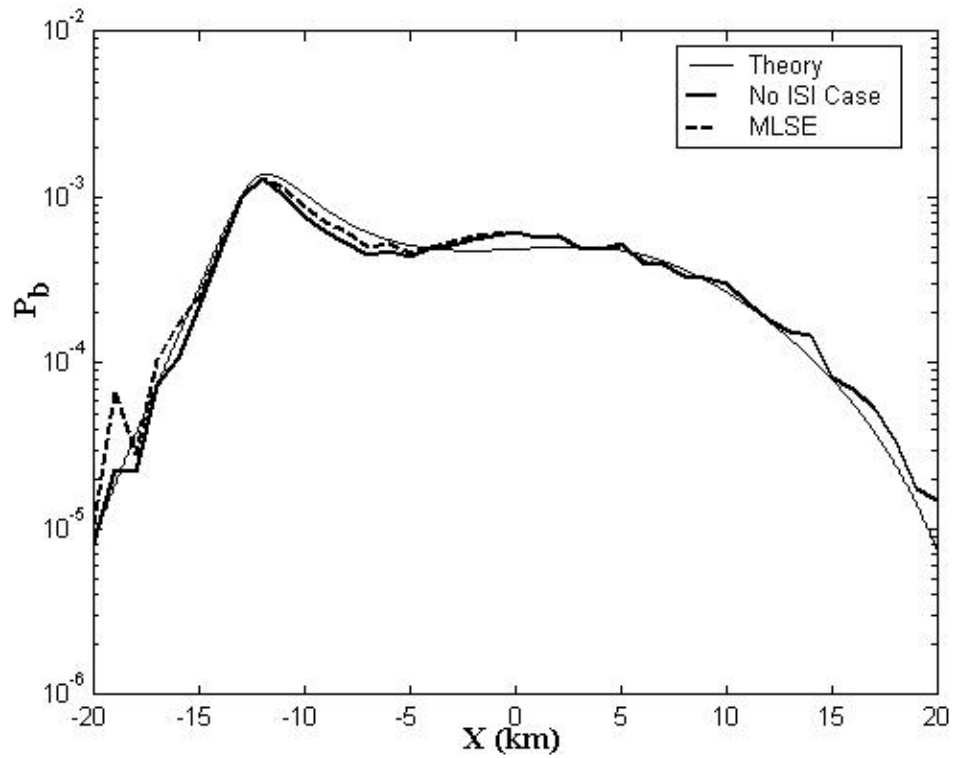

Figure-25 P_b versus mobile position with a 32-state Viterbi decoder employed in Receiver 2

6.4 Performance Evaluation at Points not on the Radial Axis

Another issue in the analysis of a simulcast network may be the performance of the scheme when mobiles are not on the line connecting a pair of base stations and when signals originating from more than two base stations are received by the mobile terminal. Obviously the performance will improve when the number of involved base stations increases since the receiver can benefit from the individual diversity paths. Let us investigate the performance on the overlap lines AO, BO and CO depicted in Figure-26 when the four neighboring base stations to each line are involved. When investigating the performance over the line AO, we consider signals received from base stations BS2, BS3, BS5 and BS6, for the line BO we consider base stations BS1, BS2, BS3 and BS5, and finally for the line CO, we consider base stations BS2, BS3, BS4 and BS5. We will investigate the performance for Receiver 2, since in the previous simulations we observed that the degradations due to both demodulation and MLSE are more significant for that receiver. We will assume a base station separation of 50 km and $\rho = 50$. From our previous evaluations, we know that a delay of two symbol periods suffices for this base station separation and SNR value. Hence, we assume $\tau = 2$ symbol periods. Note that in this case, there are two different transmit delay values for neighboring base stations on the network.

Table-4 Worst Performances on lines AO, BO and CO in LOS and Rayleigh fading environments. The mobile comprises Receiver 2.

		AO	BO	CO
Worst Case Received Energy for LOS Propagation	ε_{SUB}	0.9938	0.8354	0.7480
	$d_{\min}^2$	0.7363	0.5861	0.6708
Worst mean bit error probability for Rayleigh Fading Environment	No ISI Case	1.0713e-004	1.1659e-004	1.0058e-004
	MLSE	1.1659e-004	1.1906e-004	1.0539e-004
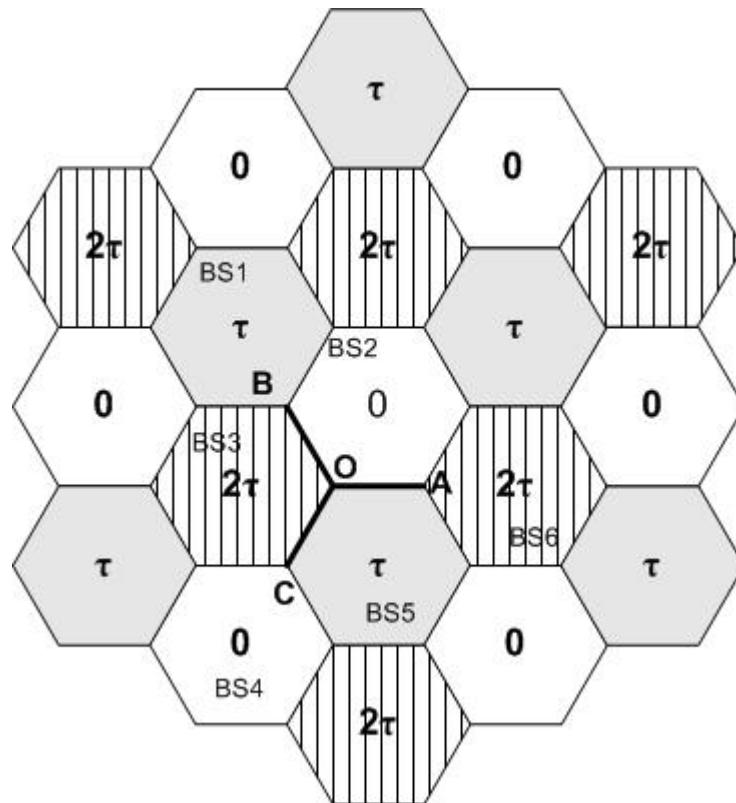
Figure-26 Performance evaluation at points not on the radial axis

Neighboring base stations on the network transmit with a relative delay of either two or four symbol periods. From Figure-23 we observe that a 32-state Viterbi decoder (L=5) is sufficient for both transmit delay values and thus assume L=5. The results are presented in Table-4. We observe that the results are close to the values obtained for the radial axis.

6.5   Comments on Performance with MLSE

In the investigations presented in this chapter we observe that the degradation in performance due to MLSE is in general more evident for Receiver 2 compared to Receiver 1. This is probably because of the fact that the whitened matched filter employed in Receiver 1 is chosen such that the overall system is minimum phase. As we stated previously the minimum phase condition implies that the energy in the first

M values of the equivalent discrete-time channel impulse response $\{f_0, f_1, \ldots, f_M, \ldots, f_L\}$ is a maximum for every M. Thus, the energy in the equivalent minimum-phase channel is mostly concentrated around f_0. The tidy and well-organized channel impulse response of the minimum phase filter reduces the probability for an error sequence, degrading d_{min}^2.

We also observe that the degradation due to MLSE is more effective for the points investigated in Section-6.4. In Table-4, worst case received energy (or equivalently) SNR drops by 1.5 dB when points on the line BO are considered in LOS propagation environment. However from Figure-23, we observe that the worst case received energy is not degraded by more than 0.5 dB for any transmit delay value when points on the radial axis are considered. On the radial axis the mobile receives signals from two base stations. Although the equivalent discrete-time channel has six taps, this means that we have actually two effective taps in the impulse response. However some parts of line BO, are in the coverage area of three base stations, which increases the number of effective taps in the equivalent discrete-time channel impulse response, meanwhile increasing the probability of an error sequence that results in degraded d_{min}^2.

Another observation is that the degradation due to MLSE is not much evident in the mean bit error probabilities for Rayleigh fading environment. As discussed in [13], the degradation due to MLSE has low probability hence the effect of the degradation on the average bit error rate is negligible. Thus, in rapidly fading environments where the average bit error rate is of interest, the transmit delay scheme can achieve the full diversity gain. However, in stationary and slow-fading environments, the effect of the degradation due to MLSE should be considered. Note also that in order to effect system performance the channels with large degradations due to MLSE should also have low energy. If the degradations occur at channels with large energies, the performance of the system will not be significantly degraded.

As a final conclusion, we may say that the degradation due to MLSE is far from exceeding the diversity gain provided to the receiver in fading environment or the

gain arising from the interference cancellation advantage of the transmit delay scheme. Thus, the scheme can be readily used for simulcasting by employing either Receiver 1 or 2 in the mobiles.

CHAPTER 7

CONCLUSION

In this thesis, a transmit delay scheme for digital simulcast environment has been investigated. The scheme has been previously suggested for simulcasting but there has been lack of knowledge about the coverage properties of the scheme. Doubts about system performance in the presence of propagation delay differences have been expressed in [3], which is the first work to suggest introducing transmit delays between base stations on a simulcast network. In fact the propagation delay differences are inevitable through out a network, resulting in coverage characteristics that may possess coverage gaps in certain regions. The coverage gaps occur in regions where the intentionally introduced delay between base stations and the propagation delay difference between different paths add up to zero. In these regions the scheme cannot provide diversity benefit to the receiver and the performance may drop significantly below the average. In that respect, a basic conclusion of this work is that the disadvantage of coverage gaps can be overcome by careful network planning. The scheme can be employed successfully for simulcast networks provided that sufficient delays are used between the base stations. In other words, by introducing sufficient delays the problem of coverage gaps can be overcome to yield smooth performance over the network. Note that "sufficient" here is in a manner of speaking "optimum" since more than sufficient delays will result in useless increased receiver complexity.

Previous studies on transmit delay strategy are all interested in providing diversity gain to a receiver in Rayleigh fading environment. However, our basic motivation in introducing the scheme is to avoid deep fades due to destructive interference at a receiver in the overlap region. By extending the relative delay between different paths in the overlap region from the order of the carrier period to the order of the symbol period, the scheme resolves the artificial multipath due to simulcasting,

turning destructive interference disadvantage into a multipath diversity advantage. This advantage of the scheme is best illustrated by considering LOS propagation between base stations and mobiles. For this reason in this thesis, we carried out the performance analysis and coverage investigations for both Rayleigh fading and LOS propagation environments.

In order to be able to investigate the performance of the scheme at different mobile locations on the network and determine the coverage properties of the scheme, in this thesis we constructed a system model that considers both propagation delay differences between different paths and the large-scale variations in the mean signal power in each path due to path loss. We have employed this model in deriving analytical bounds and performing simulations for an MLSE based coherent $\pi/4$ DQPSK receiver. We provided our results using parameters for the TETRA system; however, the results of the work can readily be used for other systems. The results show that delays of several symbol periods are sufficient for optimum performance over the network and this optimum delay value depends on network design parameters like transmitter separation and SNR.

Computer simulations for the MLSE based $\pi/4$ DQPSK receiver were carried out assuming two different demodulators at the receiver, an optimum demodulator for channels with ISI known as the whitened matched filter and a suboptimum but simplified demodulator. The suboptimum demodulator is, in fact, the optimum demodulator for the AWGN channel without ISI, which is not a valid assumption for the overall channel in our case. The results show that the receiver comprising a maximum likelihood sequence estimator at the output of the optimum demodulator completely meets the theoretical expectations and with this receiver model, the degradation in performance due to MLSE of the interfered symbol stream is not evident in our investigations. Meanwhile the receiver comprising a suboptimum demodulator and maximum likelihood sequence estimator may cause small losses in SNR (up to 0.75 dB loss in SNR, considering the worst case criteria and points on the radial axis in LOS propagation environment) provided that a sufficient state Viterbi decoder is employed at the receiver. Thus we may conclude that both receiver models can be used in the mobile terminals to obtain the full diversity gain

79

provided by the scheme. However employing the whitened matched filter at the receiver seems more advantageous since the resulting system is minimum phase in this case, hence a Viterbi decoder with less number of taps suffices.

7.1 Future Work

Although our results are promising, several interesting problems remain to be investigated when a practical simulcast network with transmit delay strategy is to be designed. In the performance investigations in this thesis we constrained ourselves to certain 'interesting' regions over the network like the radial axis connecting two neighboring base stations or the overlap line of two base stations. For the sake of simplicity most of the time, we also considered only the signals received from these two neighboring base stations. The delay to be introduced between base stations was optimized considering only these specific regions and limited paths. When a practical system is to be designed a detailed performance analysis over the whole network, considering the paths from all base stations should be carried out. The delay to be introduced between different base stations should also be optimized considering the coverage property over the whole network. In the analyses it may also be necessary to take into account the properties of the target terrain and consider phenomena like shadowing. Finding solutions for such detailed analysis will probably require sophisticated optimization algorithms, when we notice that the transmitter locations and transmitter powers are also free parameters that should be optimized.

In this thesis we considered the LOS and Rayleigh fading channels, which are accepted channels for only evaluation purposes. It may be interesting to investigate the performance of the scheme for more realistic channel models defined in the TETRA standard for urban, rural and hilly area propagation conditions. The defined channel models exhibit several discrete paths from the base station to the mobile and also include the effect of Doppler shift due to mobile movement which will increase the evaluation complexity of the scheme.

Another interesting idea may be to design a transmit delay based simulcast network with triangular cell configuration. Triangular cell configuration yields large overlap

zones between adjacent base stations. Since the scheme is capable of providing diversity gain to the mobiles in the overlap regions, triangular cell configuration may allow the design of a simulcast network with regularly spread low power transmitter sites. However wide overlap areas will result in increased length of the equivalent channel from the signal source to the receiver rendering increased receiver complexity and analysis more difficult.

REFERENCES

[1]   G. Malgren, "Single Frequency Broadcasting Networks", PhD Thesis, Department of Signals, Sensors and Systems, Royal Institute of Technology, Stockholm, Sweden, April 1997.

[2]   G. D. Gray, "The Simulcasting Technique: An Approach to Total-Area Radio Coverage", IEEE Trans. Veh. Tech. Vol. 28 pp.117-125, May 1979.

[3]   A. Wittneben, "Base station modulation diversity for digital SIMULCAST," in 41st IEEE Vehicular Technology Soc. Conf. Proc., St. Louis, USA, 1991, pp. 848–853.

[4]   U. Hansson, "Efficient Digital Communication over the Time Continuous Rayleigh Fading Channel", PhD Thesis, submitted to Chalmers University of Technology, Göteborg, Sweden, 1997.

[5]   Alejandro Moran, Fernando P. Fontan, Jose M. Hernando Rabanos and Manuel Montero del Pino, "Quasi-Synchronous Digital Trunked TETRA Performance," in IEEE Trans. Veh. Technol., vol.48, no.3, May 1999.

[6]   A. M. Alshamali and R.C.V Macario, "TETRA Performance in Quasi-Synchronous Transmission Enviroment," Personel Wireless Communications, IEEE International Conference on, Feb. 1996, pp. 227-331.

[7]   A. M. Alshamali and R.C.V Macario, "Coverage Strategy in TETRA Quasi-Synchronous Systems," Propagation Aspects of Future Mobile Systems (Digest No: 1996/220), IEE Colloquium on, Oct. 1996, pp. 3/1 - 3/6.

[8]   A. M. Alshamali and R.C.V Macario, "Performance Evaluation of TETRA in Hilly and Urban Terrain, and in Quasi Synchronous Environment," Multipath Countermeasures, IEE Colloquium on, May 1996, pp. 3/1 - 3/6.

[9] Per-Erik Östling, "Performance of MMSE Linear Equalizer and Decision Feedback Equalizer in Single-Frequency Simulcast Environment," in Proc. 43rd IEEE VTC, May 18-20 1993, pp.629-632.

[10] A. K. Salkintzis and P. T. Mathiopoulus, "On the Combining of Multipath Signals in Narrowband Rayleigh Fading Channels", IEEE Trans. Broadcasting, Vol.45, No. 2, June1999.

[11] A. Wittneben, "A New Bandwidth Efficient Transmit Antenna Modulation Diversity Scheme for Linear Digital Modulation," in Proc. IEEE Int. Conf. Communications, May 23-26 1993, pp. 1630–1634.

[12] N. Seshadri and J. H. Winters, "Two signaling schemes for improving the error performance of FDD transmission systems using transmitter antenna diversity," in Proc.1993 IEEE Vehicular Technology Conf. (VTC 43rd), May 1993, pp.508–511.

[13] J. H. Winters, "The diversity gain of transmit diversity in wireless systems with Rayleigh fading," in IEEE Trans. Veh. Technol., vol.47, no.1, Feb. 1998, pp. 119–123.

[14] P. E. Mogensen, "GSM base station antenna diversity using soft decision combining on up-link and delayed-signal transmission on down-link" in Proc. 43rd IEEE Vehicular Technology Conf., May 1993, pp.611-616.

[15] S. M. Alamouti, "A Simple Transmit Diversity Technique for Wireless Communication," IEEE Journal on Selected Areas in Communications, Vol.16, No. 8, October 1998.

[16] J. E. Mazo, "Exact matched filter bound for two-beam Rayleigh fading," in IEEE Trans. Commun., vol. 39, no. 7, July 1991, pp. 1027-1030.

[17] D. Dernikas and J.G. Gardiner, "Modelling the Simulcast Radio Transmission", IEE National Conf. On Antennas and Propagation, Conference Publication No.461, 1999.

[18] J. D. Gibson, "The Mobile Communications Handbook", IEEE Press, 1996.

[19] ETSI, TETRA, Part 2, "Air Interface", EN 300 392-2 V2.1.1, 2000-12.

[20] William C. Y. Lee, "Mobile Communications Engineering", McGraw-Hill, 1998.

[21] J. G. Proakis, "Digital Communications", McGraw-Hill, 2000.

[22] R. Steele, "Mobile Radio Communications", IEEE Press, 1996.

[23] R. Rebhan and J.Zender, "On the Outage Probability in Single Frequency Networks for Digital Broadcasting", IEEE Trans. On Broadcasting, Vol.39, No.4, Dec. 1993.

[24] G. D. Forney, "Maximum likelihood sequence estimation of digital sequences in the presence of intersymbol interference," in IEEE Trans. Commun., vol. IT-18, no. 7, pp. 363-378, May 1972.

[25] R. R. Anderson and G. J. Foschini, "The minimum distance for MLSE digital data systems of limited complexity," IEEE Trans. Inform. Theory, vol. IT-21, no.5, pp. 544-551, Sept. 1975.

[26] G. Vannucci and G. J. Foschini, "The minimum distance for digital magnetic recording partial responses," IEEE Trans. Inform. Theory, vol. 37, no. 3, pp 955-960, 1991.

[27] A. Papoulis, "Probability, Random Variables and Stochastic Processes", McGraw Hill, 1991.

[28] Schwartz, Bennett, and Stein, "Communication Systems and Techniques", McGraw Hill, 1996.

APPENDIX A

ROOT RAISED COSINE SPECTRUM

The modulation pulse $g(t)$ used in this thesis is the ideal symbol waveform, obtained by the inverse Fourier transform of a square root raised cosine spectrum $G(f)$. This is also the modulation pulse for TETRA. $G(f)$ is defined as follows[19,21]:

$$G(f) = \begin{cases} T & \left(0 \leq |f| \leq \dfrac{1-\alpha}{2T}\right) \\[2ex] \sqrt{\dfrac{T}{2}\left\{1+\cos\left[\dfrac{\pi T}{\alpha}\left(|f|-\dfrac{1-\alpha}{2T}\right)\right]\right\}} & \left(\dfrac{1-\alpha}{2T} \leq |f| \leq \dfrac{1+\alpha}{2T}\right) \\[2ex] 0 & \left(|f| \geq \dfrac{1+\alpha}{2T}\right) \end{cases}$$

where α is the roll-off factor, which determined the width of the transmission band at a given symbol rate. The value of α is assumed 0.35 in this thesis. In the derivations through out this thesis we frequently encounter the normalized auto correlation function of $g(t)$ defined as,

$$q(t) = \frac{1}{\varepsilon_g} \int g(\tau) g^*(\tau - t) d\tau \ .$$

The pulse $q(t)$, having the raised cosine spectrum, is

$$q(t) = \frac{\sin(\pi t / T)}{\pi t / T} \frac{\cos(\pi \alpha t / T)}{1 - 4\alpha^2 t^2 / T^2} \ .$$

Note that $q(t)$ is normalized so that $q(0) = 1$.

APPENDIX B

THE CHARACTERISTIC FUNCTION OF QUADRATIC FORM OF ZERO MEAN COMPLEX GAUSSIAN RANDOM VARIABLES

In this appendix, we will derive the characteristic function of a quadratic form of zero mean complex Gaussian random variables based on the references [21, Appendix B], [27] and [28, Appendix B]. We will then evaluate the characteristic function $\psi_Q(i\omega)$ of the quadratic form Q defined in Equation (32).

Let us consider a set of complex Gaussian random variables

$$\mathbf{x} = \begin{bmatrix} x_1 & x_2 & \cdots & x_n \end{bmatrix}^t$$

that have zero mean and covariance matrix

$$\mathbf{C} = \frac{1}{2} E\{\mathbf{x}\mathbf{x}^\uparrow\}$$

where $\mathbf{x}^t$ denotes the transpose of vector $\mathbf{x}$ and $\mathbf{x}^\uparrow$ denotes complex conjugate transpose of $\mathbf{x}$. The joint pdf of $\mathbf{x}$ equals

$$p_\mathbf{x}(\mathbf{x}) = \frac{1}{(2\pi)^n |\mathbf{C}|} \exp\left\{-\frac{1}{2}\mathbf{x}^\uparrow \mathbf{C}^{-1}\mathbf{x}\right\}$$

where $|\mathbf{C}|$ is the determinant of $\mathbf{C}$.

Let the quadratic form Q be

$$Q = \mathbf{x}^{\uparrow}\mathbf{D}\mathbf{x}$$

where $\mathbf{D} = \mathbf{D}^{\uparrow}$. The characteristic function of Q is:

$$\psi_Q(i\omega) = \int_{-\infty}^{\infty} \frac{1}{(2\pi)^n |\mathbf{C}|} \exp(-\frac{1}{2}\mathbf{x}^{\uparrow}\mathbf{C}^{-1}\mathbf{x}) \exp(i\omega\mathbf{x}^{\uparrow}\mathbf{D}\mathbf{x}) d\mathbf{x}$$

$$= \frac{1}{|\mathbf{I} - i\omega 2\mathbf{C}\mathbf{D}|}$$

For our problem in Section-3.4

$$Q = \frac{\rho}{2}\left(|\alpha|^2 + |\beta|^2 + 2q(\tau + \tau_p)\operatorname{Re}\{\alpha\beta^*\}\right)$$

thus

$$\mathbf{C} = \frac{1}{2}E\left\{\begin{bmatrix}\alpha\\\beta\end{bmatrix}\begin{bmatrix}\alpha^* & \beta^*\end{bmatrix}\right\} = \frac{1}{2}E\left\{\begin{bmatrix}|\alpha|^2 & \alpha\beta^*\\\beta\alpha^* & |\beta|^2\end{bmatrix}\right\} = \begin{bmatrix}p_\alpha & 0\\0 & p_\beta\end{bmatrix}$$

since α and β are independent and

$$\mathbf{D} = \frac{\rho}{2}\begin{bmatrix}1 & q(\tau + \tau_p)\\q(\tau + \tau_p) & 1\end{bmatrix}.$$

Thus,

$$|\mathbf{I} - i\omega 2\mathbf{C}\mathbf{D}| = \begin{vmatrix}1 - i\omega\rho p_\alpha & -i\omega\rho p_\alpha q(\tau + \tau_p)\\-i\omega\rho p_\beta q(\tau + \tau_p) & 1 - i\omega\rho p_\beta\end{vmatrix}$$

$$= -\omega^2 \rho^2 p_\alpha p_\beta\left(1 - q^2(\tau + \tau_p)\right) - i\omega\rho(p_\alpha + p_\beta) + 1$$

87

$$= (1 - i\omega\rho d_1)(1 - i\omega\rho d_2)$$

where

$$d_{1,2} = \frac{(p_\alpha + p_\beta) \mp \sqrt{(p_\alpha - p_\beta)^2 + 4 p_\alpha p_\beta q^2 (\tau + \tau_p)}}{2}.$$